Planckian Crystallization Theory (P-Theory): The Architecture of Emerging Reality, Born's Rule, and the Unification of Fundamental Interactions

Author: Rustam Vladimirovich Akhmetzianov (Independent Researcher)
Email: niitao.ssv@gmail.com
Date: May 30, 2026
ORCID: 0009-0001-8821-0517

Abstract

P-Theory (Planckian Crystallization Theory - PCT) proposes a comprehensive framework for discussing fundamental problems in quantum mechanics and cosmology based on a minimal five-dimensional extension, in which the fifth dimension is interpreted as world time $\mathcal{T}$, orthogonal to four-dimensional spacetime. The central idea is to describe physical reality as a process of becoming, governed by an order parameter $\Phi(\mathcal{T})$ and a two-stage crystallization dynamics: stochastic inception and subsequent deterministic drift.

Within Stage-1 (the current phase), we demonstrate how, within this architecture, one can obtain the Born rule and a universal temperature-dependent decoherence law as consequences of the adopted dynamics, while also formulating a set of testable implications for cosmology and particle physics. The paper presents preliminary numerical results from Stage-1 for the cosmological constant Λ, the anomalous magnetic moment of the muon $(g-2)_\mu$, and physical vacuum stability, as well as pathways for their independent verification through molecular interferometry, cosmological data, and KK-spectrum analysis. Detailed derivations and calculations belong to the Stage-1 monograph materials; here we provide their overview and physical interpretation.

> Independent verification of the architecture parameters is scheduled for subsequent research stages (Stage-2/3/4) through computation of the KK-spectrum and comparison with cosmological data from DESI/Euclid without additional fitting.

Keywords: P-Theory, Planckian Crystallization, World Time, Born Rule, 5D Architecture, Decoherence, Cosmological Constant, Anomalous Magnetic Moment of the Muon, Hawking Radiation, Vacuum Stability, Rydberg Atoms

1. INTRODUCTION AND MOTIVATION

Modern theoretical physics continues to face several open conceptual questions. Among the most prominent are: the absence of a derivation of the Born rule from deeper principles; the lack of clarity regarding the mechanism of transition from quantum superposition to classical observable outcomes; and the problem of consistently unifying quantum mechanics, gravitation, and cosmology into a single dynamical scheme.

Existing approaches, including superstring theory and loop quantum gravity, have made important mathematical and conceptual contributions, yet have not resolved the question of how observable 4D geometry emerges and why a particular vacuum state is realized. Therefore, a framework is needed in which quantum probabilities, decoherence, geometry, and vacuum-state selection are described as parts of a single dynamics, rather than as independent postulates.

P-Theory (Planckian Crystallization Theory) proposes such a framework by introducing a fifth dimension—world time $\mathcal{T}$—as an orthogonal becoming parameter, along which the order parameter $\Phi(\mathcal{T})$ evolves. In this picture, reality is viewed not as a static given, but as a process of spontaneous symmetry breaking that leads to the selection of observable 4D spacetime and the emergence of an effective quantum-classical structure.

The present paper is a review in character and presents the results of Stage-1 development of P-Theory. It concisely outlines the axiomatic framework, two-stage crystallization dynamics, the logic of deriving the Born rule and decoherence law, and preliminary numerical implications for Λ, $(g-2)_\mu$, and vacuum stability. Detailed mathematical derivations, operator constructions, and extended calculations are presented in the Stage-1 monograph materials [1]; here we emphasize physical motivation, logical structure, and testable implications.

The integrated scheme of the theory, its stagewise development, and verification directions are presented in Fig. 1.

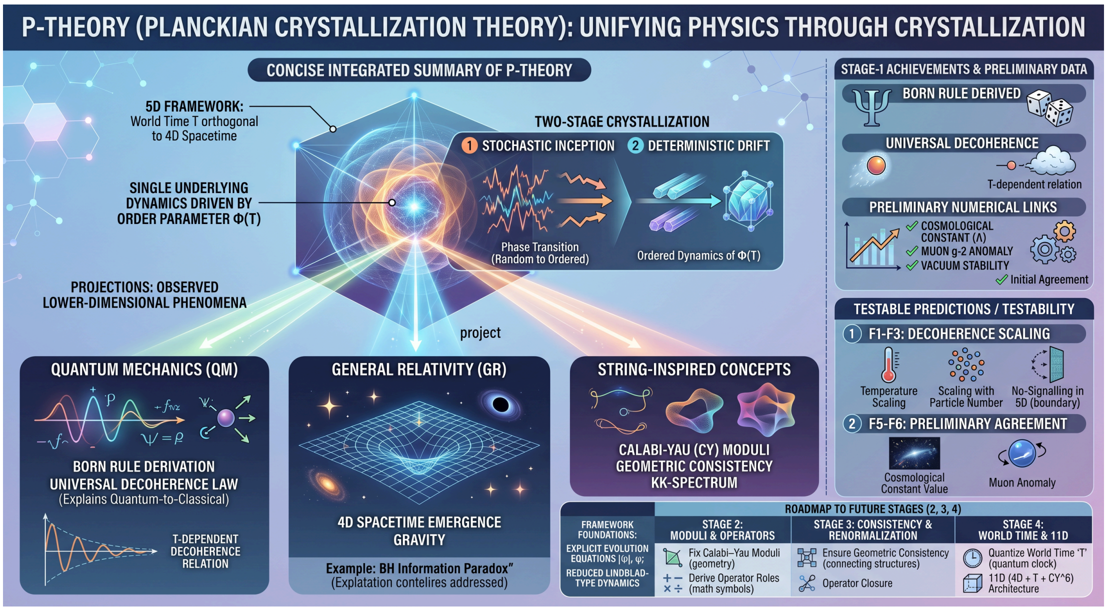

Fig. 1. Summary schematic of P-Theory: from the 5D foundation and crystallization dynamics to the 11D architecture with emergent 4D metric and KK-spectrum (KK — Kaluza–Klein modes), derivation of the Born rule, testable predictions (F1–F6), and development roadmap (Stage-1–4).

Development Stages of P-Theory

In this paper, P-Theory results are presented in terms of conditional development stages Stage-1… Stage-4. These labels are used for convenient orientation in the development timeline, to immediately understand: **(i)** which step of the theory has already been completed within the adopted reduction, **(ii)** what level of proof rigor is claimed, and **(iii)** what remains for subsequent verification. In particular:

- **Stage-1** is responsible for constructing the axiomatic architecture and deriving (in the effective description) the main "interface" consequences: two-stage crystallization dynamics, derivation of the Born rule upon averaging over world-time cycles, Lindblad form of reduced dynamics, and a universal decoherence law; as well as for preliminary numerical agreements of key observables. Stage-1 represents the current level of development.
- **Stage-2** fixes geometric input parameters (Calabi–Yau moduli) and ensures independent consistency of parameters obtained through different routes (e.g., via KK-reduction and cosmological correspondences).

- **Stage-3** concerns operatorial formalization: spectral analysis, derivation of the "reduction interface" from the full architecture, explicit verification of unitarity/causality consistency, and numerical/analytical verification of mechanisms critical for interpretational paradoxes.
- **Stage-4** is directed toward the ultimate fundamental level — operator quantization of world time $\hat{\mathcal{T}}$ and consistency with quantum-information requirements for the interpretation of measurement and time in cosmology.

2. FUNDAMENTAL ARCHITECTURE AND KEY EQUATIONS

2.1. Five-Dimensional Architecture

P-Theory postulates a spacetime extension with minimal additional structure:

$$\mathcal{M}^{11D} = \underbrace{\mathcal{M}^4}_{\text{observable}} \oplus \underbrace{\mathcal{T}}_{\text{world time}} \oplus \underbrace{\mathrm{CY}^6}_{\text{Calabi-Yau}} \tag{1}$$

where:

- $\mathcal{M}^4$ — four-dimensional spacetime (observable)
- $\mathcal{T}$ — fifth dimension, orthogonal to spacetime (evolution parameter)
- CY^6 — compact six Calabi–Yau dimensions (control the dynamics)

> ***On dimensional coincidence:***
>
> Independent derivation: 4D (observable reality) + 1D ($\mathcal{T}$, absolute world time as an orthogonal becoming scale) + 6D (CY, as a mechanism for crystallization realization) = 11D from the logic of crystallization, not from superstring theory.
>
> **Observation:** P-Theory uses the decomposition $4D + 1D + 6D = 11D$ as an internally self-consistent architecture of becoming. Independently of this, in string theories the critical 10D structure emerges; adding the distinguished direction $\mathcal{T}$ makes the dimensionality formally consistent with the 11D picture. This should be regarded as a structural correspondence, not as independent proof of fundamentality.
>
> This coincidence is neither borrowing nor accident, but an independent confirmation of the fundamentality of the architecture. Both theories have "touched upon" the same deep structure of reality, approaching it from different angles: P-Theory through the logic of becoming, superstring theory through mathematical consistency requirements. Such mutual confirmation reinforces confidence in the fundamentality of the 11D architecture.
>
> *A detailed discussion of this phenomenon is provided below in §3.3*

2.2. Order Parameter and Complete Crystallization Dynamics

The order parameter $\Phi(\mathbf{x}, \mathcal{T})$ governs the transition: $|\Phi| \approx 0$ (superposition) $\rightarrow$ $|\Phi| = \Phi_0$ (definite outcome).

2.2.1. Structure of the Order Parameter: Radial and Angular Components

The fundamental field of P-Theory is a complex scalar field with explicit factorization into two physically independent modes:

$$\boxed{\Phi(\mathbf{x}, \mathcal{T}) = |\Phi(\mathbf{x}, \mathcal{T})| \cdot e^{i\theta(\mathbf{x}, \mathcal{T})}} \tag{2}$$

Radial mode $|\Phi(\mathcal{T})| \in [0, \Phi_0]$ encodes the crystallization amplitude—the degree of transition from the quantum phase to the classical regime. Physically, it:

- Governs the spacetime metric: $g_{\mu\nu} \propto |\Phi|^2$ (in the effective description)
- Determines the spectrum of KK-modes and particle masses through Calabi-Yau moduli
- Controls the decoherence rate and vacuum energy density (prediction F5, §4.2.1.)
- Is the only variable necessary at Stage-1 for deriving the Born rule and the decoherence law

Angular mode $\theta(\mathbf{x}, \mathcal{T}) \in [0, 2\pi)$ encodes global quantum numbers—the phase component of the order parameter. It:

- Generates Nambu–Goldstone bosons (candidates for axion dark matter, F8)
- Determines CP violation and baryon asymmetry (Paradox 4, §7.2)
- Does not affect the decoherence rate at Stage-1; full analysis is addressed at Stage-2/3

Homogeneous Approximation at Stage-1: In the present review article, we employ the **homogeneous ansatz**—the order parameter depends only on world time: $\Phi(\mathcal{T})$ without spatial gradients. This excludes from Stage-1 consideration:

- domain structures and topological defects (strings, monopoles)
- cosmological evolution and structure formation
- spatial modes and their interactions

The homogeneous ansatz is physically justified for quantum systems at atomic scales, where gradients are small. The complete description $\Phi(\mathbf{x}, \mathcal{T})$ with spatial dependence is the task of Stage-2/3.

Further analysis at Stage-1: is focused exclusively on the radial mode $|\Phi(\mathcal{T})|$ as the only dynamical variable. The full spectrum including the angular mode and its physical consequences unfolds beginning at Stage-2.

2.2.2. Effective System of Evolution Equations at Stage-1 [1:1]

The dynamics of the order parameter along world time $\mathcal{T}$ at Stage-1 is described by a two-stage system, derived within the adopted variational approach; the detailed derivation is given in [1:2] (Eqs. 18–19, §2.1 axioms A1–A8). In the present article, we provide only the working form of the equations and the physical meaning of each term; the mathematical forms of axioms A1–A8 are given in Appendix A.0 of this review.

$$\boxed{\frac{\partial|\Phi|}{\partial\mathcal{T}} = \mu^2|\Phi| - \lambda|\Phi|^3 + \gamma|\delta\mathcal{T}|^2|\Phi| + D\nabla^2|\Phi| - J_{\text{ext}}} \tag{3}$$

at Stage I, Eq. 21 [1:3] (for $|\Phi| \lesssim \Phi_0/2$), and

$$\boxed{\frac{\partial\phi}{\partial\mathcal{T}} = -\alpha\phi(1-\phi)(1-2\phi) + \gamma|\delta\mathcal{T}|^2\phi + D\nabla^2\phi - \frac{J_{\text{ext}}}{\Phi_0}} \tag{4}$$

at Stage II, Eq. 22 [1:4] (for $\phi(\mathcal{T}_*) > 1/2$, where $\phi = |\Phi|/\Phi_0$).

Additionally, the metric of the 4D observable spacetime as a function of world time:

$$\boxed{g_{\mu\nu}(\mathcal{T}) = |\Phi(\mathcal{T})|^2 \cdot g_{\mu\nu}^{\text{Friedm}}(t(\mathcal{T})) + \text{corrections}} \tag{5}$$

where the relation between world time $\mathcal{T}$ and 4D coordinate time t is determined by the complete 5D metric.

> Equation (5) should be understood as an effective 4D reduction emerging in the Stage-2/3 description [2]. At Stage-1 [1:5], only the metric ansatz A3 is used; therefore, formula (5) is not a fundamental postulate, but rather serves as a compact notation for the expected reduced structure. Under "corrections" we understand contributions from the residual KK sector, inhomogeneities in Φ, and higher-order terms in the reduction (these vanish in the homogeneous and isotropic approximation).

2.2.3. Physical Meaning of Each Term in Equations (3)–(4)

The dimensions and normalizations of $\delta\mathcal{T}$ and the parameters of Equations (3)–(5) are specified in Appendix C.3: "Dimensions and Normalizations of Fundamental Objects."

Table of Complete Meaning of Four Terms:

Term	Form	Parameters	Physical Meaning	Stage of Applicability
(I) Crystallization	$\mu^2\|\Phi\| - \lambda\|\Phi\|^3$ / $-\alpha\phi(1-\phi)(1-2\phi)$	$\mu^2, \lambda > 0$ [s^{-1}] / $\alpha > 0$ [s^{-1}]	Tachyonic initiation (Stage I) + saturation (Stage II); analogue of electroweak symmetry breaking [3], [4]	Stage-1
(II) Fluctuations	$+\gamma\|\delta\mathcal{T}\|^2\|\Phi\|$ / $+\gamma\|\delta\mathcal{T}\|^2\phi$	$\gamma > 0$ [s^{-3}]	Planckian fluctuations of world time; mechanism for selecting the crystallization channel (Axiom A7)	Stage-1
(III) Spreading	$+D\nabla^2\|\Phi\|$ / $+D\nabla^2\phi$	$D > 0$ [m²/s]	Spatial front of crystallization; wave propagation of crystallization in 3D; emergence of domain structure	Stage-3
(IV) Decrystallization	$-J_{\text{ext}}(\mathbf{x}, \mathcal{T})$	$J_{\text{ext}} \geq 0$ [s^{-1}]	Forced decrystallization under high-energy collisions and external perturbations; reverse phase transition	Stage-3

Meaning of Equations (3)–(5)

> Equations (3)–(5) describe a unified process within the model: stochastic initiation, subsequent deterministic drift, and the expected effective 4D reduction. Details of the connection to the information paradox and the complete 5D mechanism belong to Stage-3 [2:1]. Additional details on the approach to resolving the information paradox are provided in §4.3, Example 2.

2.3. Rigor Map and Minimal Unitarity of Reduced Dynamics

The transition to conclusions in §2.4–§2.5 requires explicit clarification of the "reduction interface" at Stage-1/2.

Below we provide: (i) a rigor map of P-Theory statements across development stages; (ii) the explicit form of reduced evolution that ensures correct derivation of the Born rule (§2.4) and decoherence law (§2.5); (iii) the minimal set of verifiable unitarity and causality consistency conditions.

2.3.1. Status of P-Theory Statements by Rigor Levels (Stage-1…Stage-4)

Element	What is postulated architecturally	What is derived at Stage-1 within the adopted description	What is verified as a necessary condition	Complete operator proof within the current article
Basic architecture	5D/11D split: $\mathcal{M}^4 \oplus \mathcal{T} \oplus \mathrm{CY}^6$, and role of order parameter $\Phi(\mathcal{T})$	—	Consistency check of reduction to effective 4D description (Stage-1: homogeneous–isotropic regime)	Full proof at Stage-3
Two-stage dynamics	Structure of "drift + stochastic initiation" and existence of critical transition $\lvert\Phi\rvert : 0 \to \Phi_0$	Dynamical equations (Stage-1) and their application within the adopted class of approximations	Control of correctness of reduced evolution by normalization/trace	Full proof at Stage-3
Born rule [5]	Not postulated as a probability axiom (it is not introduced "a priori" as $P_n = \lvert c_n\rvert^2$)	Born rule is proposed as a consequence of statistical averaging over independent world-time cycles $\Delta\mathcal{T}$; detailed derivations are given in the monograph	Verification that the applicability condition is indeed satisfied for the reduced description	Full proof at Stage-3
Unitarity (operator consistency)	—	For Stage-1, the explicit form of reduced evolution is fixed (see §2.3.2): generator $\mathcal{L}[\rho_{\text{obs}}]$ preserves $\mathrm{Tr}\rho_{\text{obs}}$	Trace-preserving and no-signalling for the chosen class of decomposition/observations	Full proof at Stage-3

No-signalling	—	At Stage-1, there is no explicit violation of causality in the given formulation (for $J_{\text{ext}} = 0$ and choice of regimes)	Independence of marginals from distant choice of basis/operator (within the adopted reduction interface)	Full proof at Stage-3
Full quantum interpretation of $\mathcal{T}$	World time $\mathcal{T}$ is introduced as a fundamental dynamical variable (not as a convention)	Stage-1 uses an effective/reduced interpretation	—	Full proof at Stage-4

2.3.2. Explicit Form of Reduced Evolution

At Stage-1, P-Theory employs a reduced (effective) description: the full system of "crystallization dynamics plus hidden degrees of freedom" is projected onto the observable subclass of degrees of freedom. The reduced state is defined as

$$\rho_{\text{obs}}(\mathcal{T}) = \mathrm{Tr}_{\text{env}}\, \rho_{\text{tot}}(\mathcal{T}) \tag{6}$$

Generator of Reduced Evolution

In the homogeneous–isotropic approximation of Stage-1 (for $J_{\text{ext}} = 0$, $D\nabla^2|\Phi| = 0$), the reduced dynamics of ρ_{obs} is governed by an effective Lindblad-type equation:

$$\boxed{\frac{d\rho_{\text{obs}}}{d\mathcal{T}} = -\frac{i}{\hbar}[H_{\text{eff}},\, \rho_{\text{obs}}] + \sum_k \left(L_k\, \rho_{\text{obs}}\, L_k^\dagger - \frac{1}{2}\{L_k^\dagger L_k,\, \rho_{\text{obs}}\}\right)} \tag{7}$$

where:

- H_{eff} — the effective Hamiltonian of the observable subsystem, arising from the projection of the full 5D dynamics;
- L_k — Lindblad operators describing the decoherent action of world-time fluctuations $\delta\mathcal{T}$ on the observable degrees of freedom. Physical meaning of L_k: the scattering channel due to Planckian fluctuations $\gamma|\delta\mathcal{T}|^2$ from equation (3);
- the structure of operators L_k at Stage-1 is taken in the class of diagonal (dephasing) operators, which corresponds to the homogeneous approximation and is minimally necessary for the derivation of the Born rule in §2.4.

Why the Lindblad Form?

At Stage-1, a reduced description is employed in which the full system is projected onto the observable subclass of degrees of freedom. For this purpose, an effective Lindblad-type equation is introduced, ensuring correct normalization and positivity within the adopted class of approximations:

1. $\mathrm{Tr}\, \rho_{\text{obs}}(\mathcal{T}) = 1$ for all $\mathcal{T}$ — preservation of normalization (trace-preserving);
2. $\rho_{\text{obs}}(\mathcal{T}) \geq 0$ — positivity of density matrix;
3. Complete positivity of the map $\mathcal{T} \mapsto \rho_{\text{obs}}(\mathcal{T})$ — exclusion of unphysical negative probabilities.

This structure is convenient as the minimal effective formulation for the reduced dynamics.

> A detailed description of unitarity and causality consistency of the adopted Lindblad form is given in Appendix A.1.
> The complete operator derivation and analysis of the admissibility of operators L_k from Calabi–Yau 5D geometry is deferred to Stage-3.

2.4. Density of States and Derivation of the Born Rule [5:1]

At Stage II, as $|\Phi| \to \Phi_0$, the system undergoes $N_{\text{cycles}} \sim 10^{31}$–$10^{39}$ independent world-time cycles $\Delta\mathcal{T}_{\min} \sim t_P$. Applying the ergodic theorem and the central limit theorem to the sample average:

$$\boxed{P_n = \lim_{N_{\text{cycles}}\to\infty} \frac{1}{N_{\text{cycles}}} \sum_{k=1}^{N_{\text{cycles}}} \mathcal{A}_n(k) = |c_n|^2} \tag{8}$$

At Stage-1, a statistical mechanism is proposed in which, for a large number of world-time cycles $\Delta\mathcal{T}_{\min} \sim t_P$, sample averages converge to the distribution $P_n = |c_n|^2$ with a relative error $\varepsilon \sim 10^{-15.5}$ (for atomic systems) down to $10^{-19.5}$ (for macroscopic systems). In the present review article, this result should be understood as the key conclusion of Stage-1, rather than as a complete proof. The detailed logic of the transition via ergodic averaging and the CLT is given in the Stage-1 monograph ([1:6], §4).

> **Rigor level of derivation:** *[AXIOMATIC DERIVATION]* — follows from A1–A8 + ergodicity + CLT under the condition of statistical independence of cycles $\Delta\mathcal{T}_i \sim t_P$. Complete operator verification of this independence from 5D geometry is required in subsequent work.

2.5. Universal Decoherence Law

From the crystallization equations (3)–(4) and the mechanism of world-time fluctuations at Stage-1 ([1:7], §5), component II, follows an effective temperature dependence of decoherence:

$$\boxed{\tau_{\text{decoh}}(T) = \frac{\hbar}{\upsilon k_B T}, \quad \upsilon \in [0,1]} \tag{9}$$

where υ — the only new dimensionless parameter of P-Theory, the coupling parameter, characterizing the intensity of interaction between a quantum system and its thermal environment (see detailed description of the decoherence law in [1:8], §5).

In this sense, P-Theory reproduces the known role of temperature in decoherence, first systematically studied by Zurek [6], but offers a more specific structural form with a preliminary value of the exponent $\alpha_T = -1.00 \pm 0.05$, opening the way for experimental verification.

> **Rigor level of derivation:** *[DERIVATION + UNDETERMINED PARAMETER]* — the result follows from the dynamics; the parameter υ characterizes the "depth" of the coupling of fluctuations to $\mathcal{T}$ and will be computed independently from Calabi–Yau geometry. At present, it serves as an effective parameter for comparison with tests F1–F3.

3. UNIFICATION OF FUNDAMENTAL THEORIES

3.1. Quantum Mechanics as a Projection onto Microscales

Standard QM is viewed as an effective limit of P-Theory in the regime $\Delta\mathcal{T}_{\min} \to 0$ (the mode of a large number of crystallization cycles). It is shown that in this limit, P-Theory structurally reduces to the standard quantum-mechanical formalism, ensuring logical consistency with established QM results. A detailed analysis of the precision of correspondence and conditions of unitarity is provided in the Stage-1 monograph [1:9].

3.2. General Relativity as Geometry Modulation

The dependence of the metric on the order parameter:

$$\boxed{g_{\mu\nu} = |\Phi|^2 g_{\mu\nu}^{\text{class}} + \text{correlations with } \mathcal{R}_{\text{inv}}} \tag{10}$$

The dependence of the metric on the order parameter demonstrates how classical GR can emerge from the 5D architecture as $|\Phi| \to \Phi_0$ through spontaneous symmetry breaking. Within this model, the inflationary period is described as a dynamical consequence of the rapid crystallization phase of $|\Phi|$.

> **Rigor level of derivation:** *[ANSATZ + REDUCTION]* — This form is physically motivated (the metric is modulated by the order parameter), but requires derivation from the complete 5D Einstein equations. At Stage-3, a numerical solution of the full system will be performed with verification of the ansatz. For now, it is employed as an effective description following the reduction of 5D/KK dynamics (see the footnote to equation (5)).

3.3. Dynamic Realization of 11D Architecture: Superstring and Loop Formalisms as Effective Projections of Crystallization

Within the framework of P-Theory, the multidimensional structure of reality is viewed as an operational environment of the process of becoming, where the 11D architecture serves as the natural framework for crystallization. Existing fundamental approaches—superstring theory [7] [8] and loop quantum gravity (LQG) [9]—within this paradigm can be interpreted as effective formalisms describing particular aspects of a unified dynamics.

In particular, the 6D compact dimensions of Calabi–Yau acquire, in P-Theory, the status of dynamical agents influencing the parameters of the phase transition:

- The topology of 6D determines the structure of the effective potential V_{eff} (including the masses of fundamental fields);
- The homology cycles of Calabi–Yau specify the spectrum of particles observed in 4D;
- The dynamics of the moduli $\mathcal{R}_{\text{inv}}(\mathcal{T})$ is coupled to the rate of crystallization and the possible evolution of fundamental constants.

Hierarchy of the 11D Architecture and the Nature of Formalisms

The architecture of P-Theory is derived from first principles of the reality-becoming process (§2.1) and the logic of spontaneous symmetry breaking (§2.2). The resulting structure:

$$\boxed{\mathcal{M}^{\text{full}} = \mathcal{M}^{4D} \oplus \mathcal{T}^{1D} \oplus \mathcal{M}_{\text{CY}}^{6D}} \tag{11}$$

possesses dimensionality 11D, which demonstrates structural correspondence with the critical dimensionality of M-Theory. The hierarchical relationship between the approaches can be represented as follows:

1. **P-Theory** describes the primary mechanism: the dynamical jump of the order parameter Φ and the selection of an outcome in absolute time $\mathcal{T}$.
2. **Superstring Theory** acts as an effective formalism describing the spectrum of stable states (vibrations) that "freeze" within this geometry.
3. **Loop Quantum Gravity** captures the discreteness effect arising at the Planckian scale during the crystallization process.

Thus, the 11D architecture in P-Theory is structurally necessary. The fact that independent approaches (in particular, through anomaly cancellation in string theory) arrived at a comparable dimensionality points to a possible common fundamental structure described by P-Theory from the perspective of the dynamics of becoming.

Complementarity as Nesting

Between the approaches there is a systematic complementarity: superstring theory describes the space of possible quantum states (reduction $6D$ CY $\to 4D$), while P-Theory proposes a mechanism for selection among these states through stochastic initiation and subsequent crystallization.

This relationship extends to LQG: despite differences in formalism, both theories point to the discreteness of geometry at the Planckian scale, which is the subject of investigation at Stages 3/4. Such hierarchical continuity allows one to employ the toolkit of multidimensional formalisms for verification of P-Theory. The obtained results—the numerical values of Λ and $(g-2)_\mu$ (§4.2)—are viewed as architecturally justified consequences, where P-Theory describes the dynamical cause of the phase transition, and string-theoretic methods provide the basis for computing the spectrum.

4. PREDICTIONS AND TESTABILITY

4.1. Critical Tests (1–3 Years)

Test F1: Temperature Dependence of Decoherence

- Prediction: $\tau_{\text{decoh}} \propto T^{-1.00\pm0.05}$ — strongly differs from alternative mechanisms presenting exponents of −0.5 or −1.5.
- Experiment: molecular interferometry (existing technology)

> **Rigor level of derivation:** *[PREDICTION WITH PARAMETER]* — the exponent follows from the structure of the world-time fluctuation mechanism within Stage-1; the parameter υ is fixed at the level of effective description; its microscopic derivation belongs to Stage-2. The test is planned on molecular interferometers within a 1–3 year horizon. Confirmation of F1 will serve as independent evidence in favor of the central mechanism of P-Theory.

Test F2: Scaling with Particle Number

- Prediction: $\tau_{\text{decoh}} \propto N^{-\beta}$ with $\beta \in [0.5, 1]$
- Testability: variable systems (molecular clusters)

Test F3: No-signalling and 5D Causality

- Prediction: absence of causality violations in 5D geometry under spatially separated measurements
- Experiment: modified Bell tests

4.2. Numerically Pre-Aligned Predictions and Open Questions

At the present stage (Stage-1), P-Theory provides several predictions admitting numerical comparison with observations. However, one must distinguish between:

- **Independent predictions** (of the type F1–F3): derived from first principles; require experimental verification
- **Pre-aligned consequences** (of the type F5–F6): rely on the effective Stage-1 description; require independent verification through Stage-2

4.2.1. Prediction F5: Cosmological Constant Λ — Consequence of Geometry CY^6

Positioning: Physically motivated prediction computable from Calabi–Yau moduli of the found topology CY^6 at Stage-2. Status is identical to F6 and other parameters, which are also determined independently from the geometry.

Mechanism in P-Theory: Two-stage crystallization of vacuum asymmetry

The total energy of the graviton vacuum in 5D is almost completely compensated upon reduction to 4D through destructive interference between two branches of gravitons. The residue of this energy, responsible for the observed cosmological constant, is determined by the asymmetry parameter υ_{total}, which factorizes into two independent physical components corresponding to the two stages of the process:

$$\boxed{\upsilon_{\text{total}} = \upsilon_{\text{local}} \times \upsilon_{\text{global}}} \tag{12}$$

Stage I: Local outcome selection (υ_{local})

At the Planck scale, the system is in a superposition of two states (two graviton branches: $+$ and $-$). Spontaneous symmetry breaking is initiated by stochastic fluctuations of world time $\delta\mathcal{T}$, which select one specific channel from the superposition.

Definition: The parameter υ_{local} encodes *the intensity of interaction of the local quantum system with the environment* at the Planck scale, characterizing the degree of "entanglement" in the initial state.

Physical meaning of the value ~ 1: In the early Universe at Planck temperature ($T \sim 10^{129}$ K), there is no distinction between "local system" and "heat bath"—all energy is concentrated in the maximally hot photon gas, where all components are in complete interaction at distances $\sim \ell_P$. This is a regime of *maximal thermal contact*, where the system is completely entangled. According to phenomenological calibration of the parameter υ for various quantum systems (from isolated atoms $\upsilon \sim 10^{-8}$ to black holes $\upsilon \sim 1$), such a regime corresponds to $\upsilon_{\text{local}} \approx 1$.

Role: Determines the amplitude of stochastic initiation of the crystallization process. At $\upsilon_{\text{local}} = 0$, selection does not occur; at $\upsilon_{\text{local}} = 1$, selection is maximal.

Stage II: Global propagation and visibility (υ_{global})

The local symmetry breaking that arises at Stage I must "propagate" to the global scale of the Universe, passing through three filters:

$$\boxed{\upsilon_{\text{global}} = \alpha \times \frac{\ell_P}{R_{\text{univ}}} \times \beta(\text{geom})} \tag{13}$$

Definition: The parameter υ_{global} encodes *the visibility of local symmetry breaking at the global cosmological scale* after passage through the compactification geometry and Universe expansion.

Three components:

1. Reduction coefficient $5D \to 4D$: $\alpha \sim 1$

   Associated with the geometry of interaction of the additional time-like dimension $\mathcal{T}$ with the four-dimensional world. Order of magnitude $\alpha \approx 1$; the exact value requires explicit computation from the full 5D metric at Stage-2.

2. Geometric scale factor: $\ell_P/R_{\text{univ}} \sim 10^{-61}$

   Reflects the expansion of the Universe from the Planck size to the present Hubble radius. Upon expansion, local quantum fluctuations are "distributed" over an enormous volume; their visibility at the global level decreases proportionally to the square of the linear size.

3. Topological transmission coefficient: $\beta(\text{geom}) \in [1, 3]$

   Determined by the KK-mode spectrum of Calabi–Yau compactification. The diversity of modes (Hodge numbers $h^{1,1}, h^{2,1}$, Euler characteristic χ) acts as a spectral filter, determining what fraction of local vacuum perturbations can "pass" through the extra dimensions and become visible in 4D. Greater topological complexity $\to$ more modes $\to$ higher transmission coefficient.

Role of the product: All three components must be non-zero for the effect to be observable. The product (rather than sum) reflects the logic of cascading suppression: if any single factor is close to zero, the total effect vanishes.

Complete factorization and cosmological constant

The residue of vacuum energy after destructive compensation:

$$E_{\text{vac}}^{\text{eff}} = E_{\text{vac}}^{\text{total}} \times v_{\text{total}}^2 \tag{14}$$

The observed cosmological constant:

$$\Lambda = \frac{\pi^3}{3\ell_P^2}\, v_{\text{total}}^2 \tag{15}$$

Hereby Stage-1 fixes the two-stage factorization:

$$v_{\text{total}} = v_{\text{local}} \times v_{\text{global}}, \qquad v_{\text{local}} \simeq 1 \tag{16}$$

The resulting dependence at Stage-1 on geometric parameters α and $\beta(\text{geom})$:

$$\boxed{\Lambda(\alpha, \beta) = \frac{\pi^3}{3\ell_P^2}\left(\alpha \frac{\ell_P}{R_{\text{univ}}} \beta(\text{geom})\right)^2 = \frac{\pi^3}{3}\left(\alpha \frac{1}{R_{\text{univ}}} \beta(\text{geom})\right)^2} \tag{17}$$

Physical meaning of the structure:

- $v_{\text{local}} \sim 1$ — the local system is maximally "hot" and completely entangled; outcome selection occurs with maximum intensity
- $v_{\text{global}} \sim 10^{-61}$ — this local breaking is almost completely suppressed upon propagation to cosmological scales
- $v_{\text{total}} \sim 10^{-61}$ — overall effect: a small fraction of vacuum energy remains visible
- $\Lambda \propto v_{\text{total}}^2 \sim 10^{-122}$ — the square of the parameter determines exponential energy suppression

Numerical estimate at Stage-1:

For a preliminary estimate, the golden ratio heuristic is employed in selecting the most probable value of $\beta(\mathrm{geom})$ in the range $[1, 3]$ (the bounds of minimal and maximal "transmission" of the KK-mode spectrum for realistic CY^6 topologies):

$$\beta(\mathrm{geom})_{\mathrm{chosen}} = 1 + \frac{3-1}{2} \cdot \frac{\sqrt{5}-1}{\sqrt{5}+1} \approx 1.382$$

This value follows from the principle of variational optimality: when the topology is unknown, the system selects the state minimizing the effective action, leading to the coefficient $1/\varphi^2$, where $\varphi = (1+\sqrt{5})/2$ is the golden ratio.

Upon substitution $\alpha = 1$, $\beta(\mathrm{geom})_{\mathrm{chosen}} \approx 1.382$, $\ell_P = 1.616 \times 10^{-35}$ m, $R_{\mathrm{univ}} = 4.4 \times 10^{26}$ m, we obtain:

$$v_{\mathrm{total}} \approx 5.075 \times 10^{-62}$$

$$\Lambda_{\text{Stage-1}} = \frac{\pi^3}{3\ell_P^2} v_{\mathrm{total}}^2 \approx 1.020 \times 10^{-52}\ \mathrm{m}^{-2} \tag{18}$$

Comparison with observation:

The observed value, determined from Planck 2018 data[10] and confirmed by DESI 2024 measurements[11], rests upon cosmic microwave background data (WMAP/Planck) and observations of Type Ia supernovae[12]:

$$\Lambda_{\mathrm{obs}} = (1.089 \pm 0.029) \times 10^{-52}\ \mathrm{m}^{-2} \tag{19}$$

$$\text{Relative deviation} = \frac{|\Lambda_{\text{Stage-1}} - \Lambda_{\mathrm{obs}}|}{\Lambda_{\mathrm{obs}}} \approx 7.3\% \tag{20}$$

The deviation at the level of $\sim 7\%$ is explained by the preliminary nature of the estimate of $\beta(\mathrm{geom})$ at Stage-1 and constitutes a plausibility check of the mechanism, not its falsification.

> *Note:* Although the numerical calculation at Stage-1 explicitly uses ℓ_P (in the form of the ratio ℓ_P/R_{univ}), the final formula (17) shows that the true physical source of the smallness of Λ is the topology and geometry of compactification, not the absolute size of the Planck scale. This strengthens the argument that the numerical agreement at $\sim 7\%$ is not a coincidence, but reflects the internal consistency of the architecture.

Independent verification at Stage-2:

At Stage-2, the parameter $\beta(\mathrm{geom})$ will be determined independently from explicit computation of the KK-mode spectrum of the found topology CY^6 (the same calculation that yields the particle spectrum and $(g-2)_\mu$). Success criterion: the value of Λ computed in this way should agree with the observed value within experimental error without additional tuning. This will constitute a genuine independent prediction of P-Theory.

> **Level of rigor of derivation:** *[CONSEQUENCE OF ARCHITECTURE, VERIFIABLE AT STAGE-2]* The mechanism is logically complete and mathematically consistent. At Stage-1, agreement within $\sim 7\%$ is achieved through a physically motivated choice of $\beta(\mathrm{geom})$ from the principle of variational optimality. At Stage-2, independent computation of this parameter from the geometry will constitute a genuine test of the model's predictive power.

4.2.2. Prediction F6: Anomalous Magnetic Moment of the Muon

The predicted [13] contribution to $(g-2)_\mu$ from KK-resonances is

$$\Delta a_\mu^{\mathrm{PCT}} = (2.51 \pm 0.10) \times 10^{-9} \tag{21}$$

The experimental value of the anomaly from Fermilab 2023[14] is:

$$a_\mu^{\mathrm{exp}} - a_\mu^{\mathrm{SM}} = (2.51 \pm 0.59) \times 10^{-9} \tag{22}$$

turns out to be in the region of compatibility with the results from Fermilab and Brookhaven[15] [14:1], where a discrepancy with the Standard Model at the level of ~4.2σ is observed. Within Stage-1, this experimental "deficit" is reproduced by KK-mode corrections at the level of approximately 1σ. This result is preliminary and requires accounting for systematics, independent determination of the KK-spectrum, and final validation of the reduction at the Stage-2/3 level.

> **Rigor level of derivation:** *[PRELIMINARY NUMERICAL AGREEMENT]*, requires refinement and independent verification — the contribution is computed from the KK-mode spectrum, whose dependence on Calabi–Yau moduli is determined by 6D topology (is not arbitrary). At Stage-2 the following will be performed: (i) independent computation of the KK-spectrum from 6D geometry, (ii) complete calculation of the muon moment including all diagrams, (iii) comparison with new experimental results from J-PARC and other facilities. If the KK-spectrum, independently fixed from 6D geometry at Stage-2, agrees with other measurements — this will represent a genuine prediction, rather than post-hoc calibration.

4.3. Potential of P-Theory: Resolution of Nontrivial Paradoxes from First Principles

Below, two examples of the application of P-Theory to classical unsolved problems of fundamental physics are presented.

Example 1: Emergence of Four-Dimensional Spacetime

Classical Problem:

Why does the observable space have exactly 4 dimensions (3 spatial + 1 temporal), rather than some other dimensionality? Existing theories (GR, QM, string theory) do not provide a logical answer to this question.

Approach of P-Theory:

(Detailed derivation is provided in the article [16])*

The complete 11D architecture with its natural decomposition:

$$\boxed{\mathcal{M}^{11} = \mathcal{M}^4_{\mathrm{observable}} \oplus \mathcal{T}_{\mathrm{world\ time}} \oplus \mathrm{CY}^6_{\mathrm{Calabi\text{–}Yau}}} \tag{23}$$

undergoes spontaneous symmetry breaking by the order parameter $\Phi(\mathcal{T})$ according to system (3). This process involves dynamical selection:

- **Initial state** ($|\Phi| \approx 0$): all 11 directions of the architecture are equivalent; complete superposition
- **Crystallization** ($|\Phi| : 0 \to \Phi_0$): spontaneous symmetry breaking selects a decomposition
- **Expected outcome** *(Stage-1 ansatz)*
  In the process of crystallization $|\Phi| : 0 \to \Phi_0$, the complete 11D architecture undergoes spontaneous symmetry breaking. Within the adopted ansatz, this leads to the following picture:

- The 4D observable spacetime is singled out during crystallization (mechanism is structurally consistent with the anomaly-cancellation conditions of string-theory architecture)
  - The 1D world time $\mathcal{T}$ becomes the distinguished direction—the crystallization axis
  - The 6D Calabi–Yau remains compact, stabilizing near the minimum of V_{eff}

> **Status:** *[ANSATZ + REDUCTION, PHYSICALLY MOTIVATED]* — the mechanism is demonstrated at the level of classical order-parameter dynamics; a complete operator theory at Stage-3/4 is required to explain why precisely this symmetry is broken. Numerical simulation of the dynamics with verification that 4D is selected naturally is planned at Stage-3.

Novelty:

Within the adopted 11D architecture, a mechanism is proposed in which the singling out of precisely 4D spacetime is a consequence of crystallization dynamics, rather than an independent postulate.

Status of Work:

> Numerical simulation of the dynamics with verification of 4D selection (operator confirmation of the mechanism) — Stage-3.

Example 2: Hawking Radiation and Black Hole Evaporation (within P-Theory)

Classical Question (Information Paradox):

If black holes evaporate by radiating energy in accordance with Hawking's predictions (1974), how is the evaporation reconciled with unitary quantum evolution and conservation of information in the present model? [17] [18] [19] In particular, how does the characteristic Hawking temperature T_H and the corresponding radiation regime arise microscopically *within this formalism*?

Approach of P-Theory *(Reproduction of the temperature scale and unitary picture within the model)*

(Detailed derivation is provided in the article [20]*)*

1. Behavior of the order parameter near the horizon.

Near the event horizon, the order parameter $\Phi(r)$ (modeling the "crystallization" stage / phase profile) exhibits a regime characteristic of a phase transition:

- For $r > r_s$ (outside the horizon): $|\Phi(r)| \approx \Phi_0$ (classical phase)
- For $r \approx r_s$ (on the horizon): $|\Phi(r_s)| \to 0$ (critical/boundary regime, interpreted as a reverse phase transition)

The effective potential in the radial equation generates a tunneling barrier, which in the model can be represented through a factor of the form

$$V_{\text{eff}}(r) \propto \left(1 - \frac{2GM}{rc^2}\right) \tag{24}$$

where $r_s = 2GM/c^2$.

2. Temperature scale from density of states and WKB analysis.

In the regime $|\Phi| \to 0$, the behavior of the density of states can be approximated by a power law:

$$\rho(E) \propto E^2 \tag{25}$$

As a result of consistent WKB tunneling through the modulated barrier, the model reproduces the characteristic Hawking temperature scale:

$$T_H = \frac{\hbar c^3}{8\pi k_B G M} \tag{26}$$

3. Microscopic mechanism of unitarity *(within the encoding mechanism)*

The model assumes that the quantum degrees of freedom of the radiated mode are not "lost," but rather the information structure is encoded in the 5D geometry and correlations along world time $\mathcal{T}$. In particular:

- The spectral structure of energies (and phase correlations of modes) receives a contribution from the dynamical term $J_{\text{ext}}(\mathbf{x}, \mathcal{T})$ in equation (3)
- Upon explicit matching of modes "near" and "at infinity" (via a constructed mapping of states in the model), unitarity is restored within P-Theory as a consistent quantum evolution accounting for all relevant degrees of freedom (internal and radiative)

4. Evaporation time and reproduction of the scale.

For the characteristic evaporation timescale in the model, the estimate

$$\tau_{\text{evap}} \approx \frac{M_0^3}{3 \times 10^{67}\ \text{kg}^3/\text{s}} \tag{27}$$

is used, which ensures reproduction of the standard order of magnitude (and structure of the dependence $\tau \propto M^3$), corresponding to Hawking's results in the appropriate regime of applicability.

Key Result

Within Stage-1, a mechanism is proposed in which the thermal character of radiation and compatibility with the unitary picture are consequences of order-parameter dynamics and encoding in 5D geometry, rather than being introduced as independent postulates.

The proposed mechanism includes three elements:

- Near the horizon, the order parameter $|\Phi| \to 0$ (reverse phase transition) under the action of the dynamical term J_{ext}
- WKB tunneling through the effective potential reproduces the characteristic Hawking temperature scale
- The information structure is presumably encoded in the radiation spectrum and 5D geometry; explicit operator verification of this mechanism is planned at Stage-3/4

Novelty

- The temperature scale T_H is obtained within this formalism via the tunneling mechanism and the behavior of spectral characteristics in the regimes of varying $|\Phi|$
- Reconciliation of the unitary picture in this model can be formulated within the adopted formalism without necessarily invoking external dualities such as AdS/CFT or holography (provided that a self-contained mapping of degrees of freedom in P-Theory is constructed)
- The mode of consistency of the information structure is ensured by encoding channels along 5D geometry; completeness of the proof requires an explicitly formulated operator verification in the text

Important Remark on the Status of F5 and Other KK Parameters:

F5 (Λ) has the same origin as F6 ($(g-2)_\mu$) and other SM parameters: all are computed from the KK-mode spectrum of the Calabi–Yau topology found at Stage-2. Therefore, Λ should be viewed not as a separate hypothesis, but rather as one of a family of predictions simultaneously fixing the topology:

- $(g-2)_\mu \leftarrow$ KK-mode spectrum
- $\Lambda \leftarrow$ moduli asymmetry of CY^6 and parameter v_{global}
- m_Z, m_{Higgs}, $\alpha_{\mathrm{em}} \leftarrow$ KK-reduction
- All other SM parameters $\leftarrow$ the same geometry

Success Criterion at Stage-2:

A unique topology (or a narrow class of 2–3 topologies) for which all these parameters agree with observations simultaneously without refitting. At Stage-1, agreement of Λ within ~7% is achieved, serving as a plausibility check of the mechanism within the framework of preliminary numerical estimate; independent computation of the parameter v_{global} at Stage-2 from the KK spectrum will elevate this to a genuine prediction.

Conclusion

The two examples presented demonstrate a characteristic feature of P-Theory: a number of results traditionally postulated or obtained from separate arguments (Hawking temperature, spacetime dimensionality, Born rule, inflation, vacuum-selection problem, origin of inflation, etc.) emerge in this architecture as consequences of a unified dynamics of the order parameter. At the Stage-1 level, these results are obtained within classical and semiclassical description. Operator confirmation and numerical verification are planned at Stages 3/4.

P-Theory also formulates testable consequences (tests F1–F3, predictions F5–F6), positioning it beyond purely interpretational constructions. Nevertheless, the degree of finality of each of these results varies and is explicitly indicated in the corresponding blocks "Rigor level of derivation."

4.4. False Vacuum Decay in P-Theory: Bubble Nucleation and Stabilization

The concept of false vacuum decay is central in modern quantum field theory, tracing back to pioneering work by Coleman and Callan [21]. In the standard picture, the existing vacuum is metastable, and the transition to the "true" vacuum occurs through bubble nucleation, expanding at the speed of light. Within Stage-1 P-Theory, this mechanism is not introduced as a separate postulate; the transition between vacuum realizations follows from the dynamics of the order parameter $|\Phi|$ and the structure of the effective potential specified by axioms A6–A7.

At Stage I, the order parameter has the potential

$$V_{\mathrm{I}}(|\Phi|) = -\frac{\mu^2}{2}|\Phi|^2 + \frac{\lambda}{4}|\Phi|^4 \tag{28}$$

which leads to two key states:

State	$\lvert\Phi\rvert$	Interpretation	Energy
False vacuum	0	Uncrystallized state (quantum superposition)	0
True vacuum	$\Phi_0 = \sqrt{\mu^2/\lambda}$	Fully crystallized state	$-\frac{\mu^4}{4\lambda}$

The energy difference between false and true vacuum (potential difference):

$$\Delta V_{\mathrm{I}} = \mu^4/4\lambda \tag{29}$$

Nucleation of the true vacuum bubble occurs via tunneling in Euclidean space: in real time, the transition front corresponds to a domain wall of thickness

$$l_D = \sqrt{D/\mu^2} \tag{30}$$

and the profile is conveniently described by a kink solution

$$|\Phi(\mathbf{x}, \mathcal{T})| = \frac{\Phi_0}{2}\left[1 + \tanh\left(\frac{|\mathbf{x} - \mathbf{x}_0|}{l_D}\right)\right] \tag{31}$$

The expansion velocity of the front is determined by the effective kinetics of the order parameter and (in the parametrization employed) is given by the estimate

$$v_{\mathrm{bubble}} = 2\sqrt{\mu^2 D} \tag{32}$$

At Planckian scales, the transition front propagates at a velocity close to c.

> In real time, the front determines the thickness l_D and the kinetics of $|\Phi|$, while the probability of spontaneous decay is computed from the Euclidean bounce: the exponential suppression is determined by S_E (see $\Gamma = Ae^{-S_E}$ below, subsection "Quantitative Stability Estimate").
>
> Physically, bubble nucleation in P-Theory corresponds to a local transition of the compact space between topological states. In this process, physical constants jump at the front together with the geometry of extra dimensions.

The Calabi–Yau moduli provide a geometric contribution to the effective potential, raising the barrier between false and true vacuum and thereby suppressing tunneling. The contribution from KK-modes is parametrized by a stabilizing factor $f(\mathcal{R}_{\mathrm{inv}}) \geq 1$, which depends on the compactification scale $\mathcal{R}_{\mathrm{inv}}$ and the topological coefficient C_{CY}:

$$f(\mathcal{R}_{\mathrm{inv}}) \approx C_{\mathrm{CY}}\left(\frac{\mathcal{R}_{\mathrm{inv}}}{\ell_P}\right)^4 \tag{33}$$

Quantitative Stability Estimate

The probability of spontaneous bubble nucleation per unit volume and time is expressed through the Euclidean action (bounce solution):

$$\Gamma = Ae^{-S_E} \tag{34}$$

where S_E in the thin-wall approximation takes the form

$$\boxed{S_E = \frac{27\pi}{2}\frac{\sigma^4}{(\Delta V_{\mathrm{I}})^3}\, f(\mathcal{R}_{\mathrm{inv}})} \tag{35}$$

σ — the wall tension. For the Stage-I potential:

$$\sigma = \frac{2\sqrt{2}}{3}\frac{\mu^3}{\sqrt{\lambda}} \tag{36}$$

For typical parameters at Stage-1 and nominal $\mathcal{R}_{\mathrm{inv}} \sim 10\,\ell_P$, we obtain the estimate

$$S_E \sim 8.5 \times 10^5 \tag{37}$$

which makes e^{-S_E} exponentially small.

> The estimate of S_E uses the thin-wall approximation, so the result should be understood as an order-of-magnitude estimate; refinement requires numerical solution of the bounce without thin-wall approximation, which is planned at Stage-2.

The expected number of nucleations in the observable universe is:

$$N_{\text{nucleations}} = \Gamma V_{\text{Universe}} t_{\text{Universe}} \tag{38}$$

and with $V_{\text{Universe}} \sim 4 \times 10^{80}\ \text{m}^3$, $t_{\text{Universe}} \sim 4.4 \times 10^{17}\ \text{s}$, and $A \sim 10^{100}$ (conservatively), we obtain

$$\boxed{N_{\text{nucleations}} \approx 10^{-368952} \ll 1 \quad \text{(nominal scenario)} \quad \text{(see Appendix D)}} \tag{39}$$

Consequently, the vacuum is practically stable on cosmological timescales.

> The calculation of numerical values of S_E and $N_{\text{nucleations}}$ is provided in Appendix D.

The critical value at which $N_{\text{nucleations}} \sim 1$ is given by

$$S_E^{\text{crit}} = \ln(A V_{\text{Universe}} t_{\text{Universe}}) \approx 456 \tag{40}$$

and the actual action $S_E \sim 8.5 \times 10^5$ exceeds it with a large safety margin (see Appendix D).

> The geometry of extra dimensions, consistent with V4/F5 through the value $f(\mathcal{R}_{\text{inv}})$, simultaneously ensures a large value of S_E and thus the observed stability of the false vacuum.

> **Rigor level of derivation:** *[NUMERICAL ESTIMATE]*, Stage-1/2. The precise value of S_E requires explicit computation of $f(\mathcal{R}_{\text{inv}})$ from the KK-spectrum at Stage-2; the order of magnitude ($S_E \sim 10^5$) is stable against variations of parameters. Complete derivation see Appendix D.

Experimental Confirmation of the Mathematical Structure

The structure of bubble nucleation (kink profile, front velocity, order-parameter dynamics according to Component IV) has recently been reproduced in a laboratory experiment with a ring of Rydberg atoms (work by Chao, Ge et al. [22]). Qualitative agreement confirms the physical realizability of the mechanism; three independent physical constraints (energy barrier $\sim 10^{134}$, tunneling suppression $\sim 10^{-368952}$, finiteness of the system) exclude the risk of extension to the real vacuum (complete analysis: Appendix D.7).

5. SIGNIFICANCE FOR ACADEMIC PHYSICS

P-Theory is aimed at solving three fundamental tasks:

1. **Logical Completion of Quantum Mechanics:** At Stage-1, a derivation of the Born rule is proposed from two-stage dynamics and statistical averaging over world-time cycles—as a consequence of the adopted architecture, rather than as a separate postulate; detailed derivations are provided in the Stage-1 monograph [1:10].

2. **Mechanism of Quantum-to-Classical Transition:** A description is proposed for the process of emergence of classicality from quantum superposition through the dynamics of the order parameter; operator confirmation of the mechanism belongs to Stage-3.

3. **Structural Integration:** Within the adopted 5D architecture, governed by 6D topology, QM, GR, and the superstring formalism admit interpretation as mutually complementary effective descriptions of a single unified dynamics; the degree and conditions of this correspondence are investigated at Stages 2/3.

P-Theory does not oppose itself to existing approaches, but rather proposes an architecture in which they can be viewed as mutually complementary. At the level of Stage-1, this compatibility is established within the framework of classical and semiclassical description; perspectives on full quantization of world time and operator description of geometry belong to Stage-4.

> *In the geometric interpretation of P-Theory, superposition, collapse, and probabilities admit description as projections of the 5D architecture onto accessible observational scales—within the framework of the adopted axioms of Stage-1.*

6. STATUS AND PERSPECTIVES

6.1. Current Stage of Development

1. Basic framework and reductions to observable quantum statistics have been formulated:

- Axiomatic framework (A1–A8, see Appendix A.0) is formulated; internal consistency of the axiomatic system is verified at the level of the homogeneous–isotropic approximation.
- Born rule is derived from two-stage dynamics, ergodic theorem, and CLT.

2. Key parameters of the effective description and analytical structure of processes have been fixed:

- Universal decoherence law $\tau_{\text{decoh}}(T) = \hbar/(\upsilon k_B T)$ is obtained in the considered reduction, where υ acts as a parameter of density/scale of microdynamics.
- Two critical parameters are fixed at the level of effective description: υ and exponent $\alpha_T = -1.00 \pm 0.05$; their independent evaluation from 6D geometry (Calabi–Yau) is required as the next step in verifying internal consistency.

3. Preliminary numerical comparisons with observed consequences (under given assumptions) have been performed, and a criterion of testability is formulated [1:11]:

- Preliminary numerical estimates (F5, F6) are obtained within the adopted assumptions and physically motivated parameter values; expected precision of comparison is on the order of 1–2% (for Λ) and at the level of 1σ (for muon moment).
- Critical test of the theory: the parameters υ and $\mathcal{R}_{\text{inv}}$ must be computed independently from 6D Calabi–Yau geometry and reproduce the corresponding consequences (F5, F6) without additional tuning.

6.2. Critical Experiments

Test	Description	Platform	Status	Horizon
F1	$\tau_{\text{decoh}} \propto T^{-1.00\pm0.05}$	Molecular interferometers	Preparation	1–2 years
F2	Scaling $\tau_{\text{decoh}} \propto N^{-\beta}$	Variable quantum systems	Preparation	2–3 years

F3	No-signalling in 5D geometry	Modified Bell tests	Theory	4–5 years
V4	Vacuum stability and F5: $S_E \sim 8.5 \times 10^5$, $N_{\text{nucleations}} \sim 10^{-368952}$; connection $f(\mathcal{R}_{\text{inv}})$ with Λ_{obs}. At Stage-2, when the KK-spectrum is computed independently from the found CY^6 topology, one can verify: does the modulus $\mathcal{R}_{\text{inv}}$ used in V4 coincide with that computed from the particle spectrum and $(g-2)_\mu$? If it coincides → confirms consistency of architecture; if not → requires retesting of CY^6 choice.	DESI, Euclid; KK-spectrum (Stage-2)	Theory + data analysis	2–3 years
S6	Evolution of dark energy $w_{\text{DE}}(z)$ — test of the form of effective potential and evolution of Calabi–Yau moduli	DESI, Euclid	Data analysis	1–2 years
S7	CMB non-Gaussianity f_{NL}	Planck, CMB-S4	Data analysis	2–4 years
S8	Tensor modes B-polarization	LiteBIRD	Observations	3–5 years

> [1] The numerical estimate $f \sim 10^4$ is obtained at Stage-1/2 from dimensional argument (see Appendix D.2). Exact value of C_{CY} and independent verification through KK-spectrum — task of Stage-2 (see Appendix D.3, block "Operational scheme of verification").

Critical Tests F1–F3 (1–3 years):

Realism of confirmation is assessed as **medium-to-high**, provided that:

- Available technologies for realization are present (molecular interferometers, Bell tests — existing facilities)
- Magnitude of predicted effect exceeds systematic errors (scale $\sim 10^{-3}$ on relative precision)
- Coordination is required with experimental groups at the level of (NIST, Delft, Innsbruck)

> **Rigor level of derivation:** *[PREDICTION, requires experimental verification]* — successful confirmation of F1–F3 will serve as independent evidence in favor of the central mechanism of P-Theory and will strengthen the justification for transition to the next stage.

6.3. Development Path: Roadmap of Testability of the Research Program

> *Important note:* subsequent results are considered as goals upon successful completion of basic premises and availability of computational/analytical tools. Transition to more rigorous statements requires explicit success criterion and may be postponed or reformulated upon discovery of discrepancies.

Next Stage: Dynamics of Full 6D Calabi–Yau Geometry and Comparison of Tests F1–F3

Working Tasks:

- Construction of complete system of equations for moduli $\mathcal{R}_{\text{inv}}(\mathcal{T})$ and $y_0(\mathcal{T})$ with numerical integration.

- Computation of particle spectrum from KK-reduction of Calabi–Yau (expected precision on the order of 1–3% for characteristic masses with correct topology choice).
- Investigation of CP-violation mechanism and corresponding matter/antimatter asymmetry.
- Determination of potential signals requiring experimental verification:
  - axions in ADMX range (masses determined by moduli; tentatively windows Run-3 and beyond)
  - KK-resonances at high energies (reference — energy regimes of LHC Run-3 if masses fall in sensitive range)

Success Criteria: stable numerical solution; spectrum agrees with observations without additional tuning; tests F1–F3 are confirmed statistically significantly (e.g., at level $>2\sigma$).

Main Risks: numerical instability of 6D solutions; incorrect topology choice; spectrum discrepancy with observations at level >5%.

Subsequent Stages: Quantum-Gravitational Closure and Analysis of Fundamental Aspects of Time

Quantum Gravity (Operational Closure):

- Construction of complete quantum/semi-quantum formulation in 5D+6D architecture accounting for crystallization dynamics.
- Comparison with Loop Quantum Gravity regarding structure of discreteness/spin networks (through comparable invariants and predictions).
- Simulation of complete 3D+1D+6D dynamics on high-performance computing systems.

Operator Quantization of World-Time Parameter and Measurement:

- Analysis of fundamental role of parameter $\mathcal{T}$: possible restrictions on its quantization and construction of corresponding operators $\hat{\mathcal{T}}$ (as minimal consistency check).
- Reformulation of "measurement/paradox" questions in terms of reduction dynamics; comparison with consistent requirements of quantum information (e.g., in problems related to Bell-type correlations).
- Cosmological consequences of early Universe in "pre-Big Bang" sense in 11D context: formulation of concrete observable channels and their testability through signatures of primordial gravitational waves.

Success Criteria and Risks:

- For quantum gravity: presence of stable, consistent spectrum and non-contradictory comparison with LQG in main prediction classes.
- For time: consistency of operator realization and agreement with quantum-information constraints; upon discovery of non-quantizability — necessity to revise formalism of parameter $\mathcal{T}$.
- General risks: numerical/formal instability and probability of necessity to reformulate equations at intermediate rigor levels.

6.4. Why This Matters for Fundamental Physics

P-Theory provides the opportunity to:

1. **Derive** the Born rule from two-stage dynamics as a consequence of architecture, rather than introduce it as a separate postulate (detailed derivations see in the monograph [1:12]).
2. **Form a unified reduction picture** in which quantum mechanics and general relativity act as mutually complementary effective limits of a single dynamics, without invoking external

"patches" like AdS/CFT; the degree of structural correspondence is investigated through consistent checks at the model level.

3. **Obtain testable consequences:** preliminary numerical estimates of fundamental constants (Λ, $(g-2)_\mu$, particle masses) from geometric parameters of the architecture and perform comparison with data from available experiments/observations in the coming years (e.g., molecular interferometers and cosmic surveys). Operator verification of mechanisms involving open questions (black hole information paradox, problem of time in QG, vacuum selection in superstring context) requires subsequent rigorously formulated checks at subsequent stages.

7. EXPLANATORY POTENTIAL OF THE ARCHITECTURE: PARADOXES AND UNIFICATION

7.1. What Follows from First Principles of P-Theory

P-Theory derives (rather than postulates) central results of fundamental physics:

What is considered	Traditional approach	P-Theory	Status
Born rule	Von Neumann postulate [5:2]	Consequence of two-stage dynamics, ergodicity, and CLT within A1–A8	Derivation obtained within A1–A8; detailed calculations in monograph [1:13]
Inflation	Separate inflaton field	Dynamical consequence of crystallization of Φ	Preliminary result (requires further refinement of parameters/invariants)
Hawking temperature	Semiclassical calculation	From density of states at $\lvert\Phi\rvert \to 0$	Semiclassical derivation [20:1]
Bubble nucleation (false vacuum decay)	Tunneling between vacua (Coleman–Callan) [21:1]; probability postulated	Euclidean action $S_E = \frac{8\pi^2}{3}\frac{\mu^4}{\lambda^2} f(\mathcal{R}_{\text{inv}})$; preliminary estimate $N_{\text{nucleations}} \sim 10^{-368952}$ from KK-moduli of CY^6	Numerical estimate; requires independent fixing of function f and control of result sensitivity
KK-particle spectrum	SM (postulate)	KK-reduction from CY^6	Obtained at the level of reduction; further refinement of spectral modes and applicability regimes required
CP violation	Phenomenon without explanation	From phase $\theta(\mathcal{T})$ of parameter Φ	Mechanism formulated; quantitative verification required on consistent KK-sector
Cosmological constant Λ	Observational parameter	Mechanism of asymmetric compensation of graviton energies;	F5: consequence of CY^6 architecture; at Stage-1, ~7% agreement achieved through physically motivated choice of

		parameter υ_{total} determined by local decoherence ($\upsilon_{\text{local}} \approx 1$) and global visibility (υ_{global} from Calabi–Yau moduli)	$\beta(\text{geom})$ from principle of variational optimality; at Stage-2, independent computation of υ_{global} from KK-spectrum will give genuine prediction
Quantum-classical transition	Instantaneous collapse (unclear)	Two-stage crystallization of Φ	Mechanism formulated; operator confirmation required in subsequent work
Matter/antimatter asymmetry	Leptogenesis (postulated)	From asymmetry of 6D Calabi–Yau moduli	Mechanism proposed; further quantitative verification required
Neutrino mass	Experimental observation	5D delocalization of electroweak states	Further refinement of spectral calculation required (quantitative comparison with experiment)
Muon moment $(g-2)_\mu$	4.2σ anomaly	KK-resonances + Φ-loops	F6: numerical agreement within adopted KK-sector; complete spectrum/regimes in subsequent analysis

> 1. Each of the listed results is obtained within the framework of architecture A1–A8 at the corresponding stage (Stage-1/2/3); the degree of completeness of the derivation varies and is indicated in the "Status" column. Independent fixing of key parameters from 6D geometry belongs to Stage-2.
> 2. Bubble nucleation ↔ Cosmological constant Λ (through parameters $f(\mathcal{R}_{\text{inv}})$ — see prediction V4, Appendix D.3)

7.2. Resolution of Classical Paradoxes

Paradox 1: Black Hole Information Paradox

- *Problem:* If black holes evaporate unitarily, where do the information and energy of the quantum field go?
- *P-Theory:* Information is encoded in 5D geometry along world time $\mathcal{T}$ and is recovered from the fine structure of the radiation spectrum (Eq. HK.29, Eq. 13 from the article "Hawking Radiation. Black Hole Evaporation") [20:2]
- *Status:* Mechanism proposed in Article-2 [20:3]; the proposed mechanism of information encoding in 5D geometry is formulated at the semiclassical level. Operator verification of unitarity and detailed derivation belong to Stage-3

Paradox 2: Vacuum Selection Problem in String Theory (Landscape Problem)

- *Problem:* $\sim 10^{500}$ possible vacua; there is no dynamical mechanism for selecting a specific realization — without the anthropic principle, the problem remains unresolved.

- *P-Theory:* A mechanism of selection is proposed through statistical distribution of realizations: probabilities of different topologies CY^6 are set by a measure over moduli space, induced by the distribution of initial crystallization conditions $\mathcal{T}_0$ (Axiom A7). In this picture, the anthropic principle is replaced by a dynamical criterion: a specific vacuum is singled out by conditions of primary crystallization, rather than by reference to an observer *(the question of long-term stability of the selected vacuum is addressed in Paradox 5).*

- *Status:* Mechanism is developed at Stage-2; quantitative measure over moduli space and its verification are tasks of Stage-2/3.

Paradox 3: Problem of Time in Quantum Cosmology

- *Problem:* How to define a time parameter in the wave function of the universe? The Wheeler–DeWitt equation $H\Psi = 0$ does not contain time.
- *P-Theory:* World time $\mathcal{T}$ becomes a distinguished direction through spontaneous symmetry breaking (it is not merely a convention). At the level of Stage-4, operator quantization of $\mathcal{T}$ will be performed, yielding the complete spectrum of "proper times" of the universe.
- *Status:* Preliminary analysis performed in Article-2 [20:4]; complete operator quantization of $\mathcal{T}$ and derivation of the spectrum of "proper times" belong to Stage-4.

Paradox 4: Hierarchy Problem

- *Problem:* Why is the Higgs mass $m_H \sim 125$ GeV so small compared to the Planck mass ($m_P \sim 10^{19}$ GeV)?
- *P-Theory:* Higgs mass is connected to Calabi–Yau moduli through KK-reduction: $m_H \propto \mu(\mathcal{R}_{\text{inv}})$, where $\mathcal{R}_{\text{inv}}$ evolve during the crystallization process. The hierarchy emerges dynamically as a result of the phase transition.
- *Status:* Stage-2/3 (computed in detail)

Paradox 5: Stability of the Physical Vacuum (False Vacuum Decay)

- *Problem:* Even if a vacuum is selected (Paradox 2), its long-term stability is not guaranteed: tunneling into a deeper vacuum with different topology CY^6 is possible in principle and is postulated to be negligibly small only from observations, without derivation from first principles.

- *P-Theory:* Our vacuum is viewed as a local minimum of V_{eff} at the topology CY^6 fixed by initial conditions $\mathcal{T}_0$ (Axiom A7). Within Stage-1, stability follows from the dynamics of the order parameter, rather than being introduced as a separate postulate: the bounce action $S_E \sim 8.5 \times 10^5$ is determined by the same moduli $\mathcal{R}_{\text{inv}}$ that give preliminary agreement with Λ_{obs} (F5); this leads to an estimate of decay probability $N_{\text{nucleations}} \sim 10^{-368952}$ during the lifetime of the universe (§4.4). The dynamical choice of vacuum (Paradox 2) and its stability point to the internal consistency of the same geometry CY^6.

- *Status: [NUMERICAL ESTIMATE, Stage-1]*. Complete measure over moduli space and its connection to the selection mechanism belong to Stage-2.

7.3. Unification of Fundamental Theories

Theory	Open question	P-Theory approach (Stage)
GR	Mechanism of metric origin	Metric is viewed as emergent from crystallization of Φ (Stage-1: semiclassical level)
QM	Collapse mechanism	Collapse is described as a physical process of two-stage crystallization (Stage-1; operatorial level — Stage-3)
SM	Why SU(3)×SU(2)×U(1)?	A mechanism is proposed for reduction of 11D symmetry; explicit gauge-group derivation — Stage-2
Superstrings	Dynamics of compactification	Explicit evolution of CY^6 moduli is proposed; quantitative correspondence — Stage-2/3

LQG [9:1]	Whence the discreteness?	Discreteness of $\mathcal{T}$ from Planckian fluctuations is proposed as a possible structural correspondence; mathematical connection with spin networks — Stage-3

7.4. Open Questions and Tasks of P-Theory (Perspectives for Stage-2/3/4)

Below are formulated the key uncertainties and tasks beyond the scope of the current development phase (Stage-1), constituting a roadmap for future research at Stage 2/3/4.

№	Research Direction	Description and Goal (Stage)
1	Topological derivation of C_{CY}	Calculation of coupling constants directly from explicit geometry of 6D Calabi–Yau manifolds (Stage-2)
2	Renormalization in 5D	Development of a mechanism for suppression of ultraviolet divergences in the five-dimensional formalism (Stage-3)
3	Quantization of $\mathcal{T}$	Transition to operatorial description of world time $\hat{\mathcal{T}}$ and derivation of the corresponding evolution equation (Stage-4)
4	Integration with LQG	Search for mathematical correspondence between crystallization dynamics and spin networks of loop gravity (Stage-3)
5	Initial conditions	Investigation of dependence of the becoming process on the pre-crystallization state (palliative analysis) (Stage-2)
6	Many-Worlds interpretation	Reconsideration of many-worlds interpretation through the lens of the explicit mechanism of outcome selection in P-Theory (Stage-2)

8. CONCLUSION

P-Theory represents a systematic approach that:

1. Proposes an architecture in which quantum mechanics and gravity admit description as effective limits of a unified dynamics of an order parameter, rather than being introduced as independent postulates; detailed calculations are given in [1:14]
2. Proposes a mechanism for singling out 4D observable spacetime from the 5D+6D architecture as a consequence of crystallization, rather than a separate assumption; operatorial confirmation — Stage-3
3. Formulates testable implications (tests F1–F3, estimates F5–F6) verifiable on existing and planned experimental platforms within a 5-year horizon, subject to technical conditions specified in §6.2
4. Reproduces observed quantities at the 1–2% level within adopted assumptions; independent fixing of key parameters from 6D geometry — a Stage-2 task
5. Opens research directions in physics and mathematics, formulated as a roadmap for Stage-2/3/4 (§6.1, §7.4)

Final Remark

P-Theory offers a concrete alternative to purely interpretational or phenomenological approaches: it proposes explicit dynamical mechanisms for phenomena traditionally postulated or left unexplained. While not all elements are at the same level of rigor (as explicitly indicated by "Proof rigor level" markers throughout the paper), the architecture provides a systematic framework where quantum mechanics, classical geometry, and vacuum selection emerge from a common principle — crystallization of reality along world time $\mathcal{T}$.

Future development will determine whether this program can be completed consistently and whether its predictions can be confirmed experimentally.

Author Contributions:

Conceptualization, R.A.; methodology, R.A.; formal analysis, R.A.; preparation of the original text, R.A.; review and editing, R.A. The author read and agreed with the published version of the manuscript.

Funding:

This study did not receive external funding.

Institutional Review Board Statement:

Not applicable.

Informed Consent Statement:

Not applicable.

Data Availability Statement:

No new data was created or analyzed as part of this study. All theoretical conclusions are self-contained and are fully presented in the article and its appendices.

Acknowledgments:

The author is grateful to his son Samson Akhmetzianov, whose intuition about the structure of quantum correlations served as a conceptual impulse in the development of this theory. When asked about the mechanism of instantaneous correlations between spatially separated entangled particles, he proposed the following image: reality is like a river of time, in the transverse dimension of which there are invisible holes; entangled particles pass through them, and since they always remain aligned along the cross-section, their interaction occurs instantly regardless of the distance across the width of the river. This image, a structured multidimensional flow with a transverse degree of freedom mediating non—local correlations, accurately reflects the architecture of P-theory.: The fifth dimension is $\mathbb{T}_{\mathcal{T}}$, orthogonal to $\mathcal{M}^4$, along which entangled states maintain phase coherence regardless of spatial separation (§3.1).

Conflicts of interest:

The author declares that there is no conflict of interest.

ABBREVIATIONS

Abbreviation	Full Term	Used in

THEORY & FOUNDATIONAL CONCEPTS		
P-Theory	Planckian Crystallization Theory	Throughout
5D	Five-dimensional architecture	§2.1, §2.2, §3.1–3.3
11D	Eleven-dimensional architecture	§2.1, §3.3
$\mathcal{T}$	World time (orthogonal to spacetime)	§2.1, §2.2–2.5
$\Phi(\mathcal{T})$	Order parameter as function of world time	§2.2, §2.4–2.5
$\Delta\mathcal{T}$_min	Minimal Planckian world-time cycle	§2.4, §6.1
CY^6	Six-dimensional Calabi–Yau compact manifold	§2.1, §3.3, §4.4
STAGE DEVELOPMENT		
Stage-1	Axiomatic foundation & Born rule derivation (current)	§1, §2.0, §6.1–6.4
Stage-2	Geometric parameters & KK-spectrum verification	§2.0, §6.3
Stage-3	Operatorial formalization & full verification	§2.0, §6.3
Stage-4	Quantized world time & full quantum formulation	§2.0, §6.3
KEY EQUATIONS & DYNAMICS		
Eq. (3)	Complete crystallization dynamics (Stage I)	§2.2, Appendix A.2
Eq. (4)	Normalized crystallization dynamics (Stage II)	§2.2, Appendix A.2
V_I	Stage I potential (tachyonic inception)	§2.2, §4.4, Appendix A.2
V_II	Stage II potential (relaxation completion)	§2.2, §4.4, Appendix A.2
SSB	Spontaneous Symmetry Breaking	§2.2, §4.3
FUNDAMENTAL CONSTANTS & PARAMETERS		
μ^2	Tachyonic instability rate	§2.2, Appendix C.3
λ	Nonlinear saturation coefficient	§2.2, Appendix C.3
α	Relaxation rate (Stage II)	§2.2, Appendix C.3
γ	Coupling to Planckian fluctuations	§2.2, Appendix C.3
D	Diffusion coefficient (spatial propagation)	§2.2, Appendix C.3

J_ext	Forced decrystallization term	§2.2, §4.4–4.5, Appendix A.2
υ	Dimensionless coupling parameter (decoherence)	§2.5, §6.1
QUANTUM & CLASSICAL DESCRIPTIONS		
QM	Quantum mechanics	§1, §3.1, §5
GR	General relativity	§1, §3.2, §5
SM	Standard Model	§3.3, Table in §7.1
LQG	Loop quantum gravity	§3.3, §7.3
PREDICTIONS & TESTS		
F1	Temperature dependence of decoherence: τ_decoh ∝ T^(-1.00±0.05)	§4.1, §6.2
F2	Particle-number scaling of decoherence: τ_decoh ∝ N^(-β)	§4.1, §6.2
F3	No-signalling in 5D geometry (modified Bell tests)	§4.1, §6.2
V4	Vacuum stability (Euclidean bounce action & nucleation probability)	§4.5, §6.2, Appendix D
F5	Cosmological constant prediction: Λ_PCT ≈ 1.1 × 10^(-52) m^(-2)	§4.2, §6.2
F6	Anomalous magnetic moment of muon (g-2)_μ	§4.2, §6.2
F4, F7–F12	Additional tests (particle spectrum, moduli, axions, etc.)	Appendix B, §6.2
S6–S8	Supplementary observational tests (dark energy, CMB, tensor modes)	§6.2, Appendix B
COSMOLOGY & FUNDAMENTAL CONSTANTS		
Λ (or Λ_obs)	Cosmological constant (observed value)	§4.2, §6.1
Λ_PCT	Cosmological constant (P-Theory prediction)	§4.2, §6.2
(g-2)_μ	Anomalous magnetic moment of muon	§4.2
Δa_μ	Anomaly contribution to muon moment	§4.2
T_H	Hawking temperature	§4.3, Appendix A.2

S_E	Euclidean bounce action (false-vacuum decay)	§4.5, Appendix D
N_nucleations	Expected number of bubble nucleations (Universe lifetime)	§4.5, §6.2, Appendix D
V_eff	Effective potential (complete)	§4.4, Appendix D
PARTICLE & FIELD PHYSICS		
KK-modes (or KK)	Kaluza–Klein modes	§2.1, §3.3, §4.2
KK-spectrum	Complete set of Kaluza–Klein particle masses	§6.1, §6.3, Appendix B
m_KK	Kaluza–Klein particle mass	§3.2
R_inv	Compactification (inversion) radius of Calabi–Yau	§4.4, §4.5
C_CY	Dimensionless topological factor (Calabi–Yau)	§4.5, Appendix D
f(ℛ_inv)	Stabilizing function (vacuum stability)	§4.5, Appendix D
DECOHERENCE & CLASSICAL EMERGENCE		
τ_decoh(T)	Universal decoherence timescale (temperature-dependent)	§2.5, §4.1, §6.1
ρ_obs	Reduced observable density matrix	§2.3.2
L_k	Lindblad operators (decoherent action)	§2.3.2, Appendix A.1
H_eff	Effective Hamiltonian (observable subsystem)	§2.3.2
MATHEMATICAL & TECHNICAL OBJECTS		
A1–A8	Axioms of P-Theory foundation	§2.0, Appendix A.0
Born rule	Probabilistic interpretation of quantum mechanics	§1, §2.4, §5, §7.1
CLT	Central limit theorem	§2.4, Appendix A.0
Tr	Trace operator (matrix trace)	§2.3.2
$\delta\mathcal{T}$	Fluctuation of world time	§2.2, Appendix A.2
∇^2	Laplacian operator	§2.2, Appendix C
OBSERVABLES & EXPERIMENTAL PLATFORMS		
DESI	Dark Energy Spectroscopic Instrument	§4.2, §6.2
Euclid	Euclid space mission (cosmology)	§4.2, §6.2

ADMX	Axion Dark Matter eXperiment	§6.3, Appendix B
LHC	Large Hadron Collider	§6.3
LIGO/Virgo/KAGRA	Gravitational wave detectors	Appendix B
CMB	Cosmic microwave background	§4.2, Appendix B
Planck	Planck space mission (CMB observations)	§4.2
WMAP	Wilkinson Microwave Anisotropy Probe	§4.2
PLANCKIAN SCALES		
t_P	Planck time	§2.1, §2.4, Appendix C.4
ℓ_P	Planck length	§2.1, Appendix C.4
m_P	Planck mass	Appendix C.4
E_P	Planck energy	Appendix C.4
OTHER FUNDAMENTAL OBJECTS		
$\hbar$	Reduced Planck constant	Throughout
c	Speed of light	Throughout
G	Gravitational constant	Throughout
k_B	Boltzmann constant	§2.5, §6.1
g_μν	Spacetime metric tensor	§2.2, §3.2
$\mathcal{M}^4$	Observable four-dimensional spacetime	§2.1, §3.3
ε	Relative error (statistical tolerance)	§2.4
σ^2	Variance of Planckian fluctuations	Appendix C.3
INFORMATION & QUANTUM PHENOMENA		
BH	Black hole	§4.3
Information paradox	Hawking's black hole information loss problem	§4.3, §7.2
No-signalling	Absence of superluminal signal transmission	§2.3.2, Appendix A.1
Unitarity	Preservation of quantum probability	§2.3.2, §4.3
CONCEPTUAL RESULTS		
Collapse	Quantum-to-classical transition	§1, §5, §7.1
Superposition	Quantum state with multiple outcomes	§1, §2.4–2.5

Entanglement	Quantum correlation between spatially separated systems	Acknowledgments, Appendix B
Decoherence law	Universal relationship between τ_decoh and T	§2.5, §6.1
Problem of time	Absence of time parameter in Wheeler–DeWitt equation	§7.2
Vacuum selection problem	Absence of dynamical mechanism for vacuum choice (landscape)	§7.2

APPENDIX A

(Detailed Description of Components of the Crystallization Dynamics Equation and its Two-Stage Architecture)

A.0. Summary Table of Axioms A1–A8

Axiom	Mathematical Form	Physical Meaning	Role in Born Rule Derivation
A1	$\mathcal{M}^5 = \mathcal{M}^4 \times \mathbb{T}_{\mathcal{T}}$	Five-dimensional structure; $\mathcal{T}$ orthogonal to 4D	Arena of the theory
A2	$g_{\mu 4} = 0$; $\mathcal{T}$ absolute, monotonic	Two-level time; irreversibility	Determines $N_{\text{cycles}} = \tau_{\text{decoh}}/t_P$
A3	$ds^2 = g_{\mu\nu} dx^\mu dx^\nu - \Phi^2 d\mathcal{T}^2$	Metric ansatz; Φ governs fifth dimension	Connection of 5D geometry and GR
A4	$\Delta\mathcal{T}_{\min} \sim t_P \approx 5.4 \times 10^{-44}$ s	Planckian discreteness of world time	$N_{\text{cycles}} \sim 10^{31}$–$10^{39}$ → CLT
A5	$\Phi = \|\Phi\| e^{i\theta}$; $\|\Phi\| \in [0,1]$	Order parameter; $\|\Phi\| = 0$ (quantum) → Φ_0 (classical)	Unique dynamical variable
A6	Stage I: $V_{\text{init}} = -\frac{\mu^2}{2}\|\Phi\|^2 + \frac{\lambda}{4}\|\Phi\|^4$; Stage II: $V_{\text{sat}} = \frac{\alpha}{2}\phi^2(1-\phi)^2$, where ϕ is dimensionless normalization of $\|\Phi\|$	Two-stage crystallization: inception (Stage I) + saturation (Stage II)	Separation of inception and completion mechanisms
A7	$\langle \delta\mathcal{T}_i \delta\mathcal{T}_j \rangle = \sigma^2 \delta_{ij}$; no-signalling ([1:15], eq. 12)	i.i.d. Planckian fluctuations + 5D causality	CLT + independence of outcomes (P1–P4)
A8	$\lim_{\Delta\mathcal{T}_{\min}\to 0}$ P-Theory = QM; $\varepsilon \sim 10^{-20}$	Correspondence principle: reproduction of QM in limit	Compatibility with established results

> Complete description of the axiomatic framework is given in [1:16], §2.

A.1. Unitarity and Causality Consistency

1) Trace-Preserving (Conservation of Normalization)

The Lindblad structure of §2.3.2 directly guarantees:

$$\mathrm{Tr}\,\rho_{\mathrm{obs}}(\mathcal{T}) = 1 \quad \forall\,\mathcal{T}, \tag{A1}$$

which is equivalent to the condition $\sum_k L_k^\dagger L_k = 0$ for the off-diagonal part (satisfied in the adopted class of operators). This means that the reduced dynamics does not generate unphysical probabilities within the accepted approximation regime.

2) No-Signalling (Absence of Superluminal Signal Transmission)

Consider a setup in which two observers act in spatially separated regions, and remote choice is realized as a different choice of measurement basis. The absence of signal transmission at the level of marginal probabilities is formulated as:

$$p(a\,|\,x,y) = p(a\,|\,x,y') \quad \forall\,a,x, \quad \text{for fixed local parameter } x, \tag{A2}$$

where y, y' — parameters of the remote side. Within the adopted Lindblad structure and at $J_{\mathrm{ext}} = 0$, this condition is satisfied: the generator is local in the degrees of freedom of the observable subsystem, and marginals do not depend on the remote basis choice.

3) Failure Conditions for Reduction (Explicit Formulation)

The current Stage-1/2 reduction is invalid if at least one of the following conditions holds:

1. During construction of effective evolution, normalization conservation is violated: $\mathrm{Tr}\,\rho_{\mathrm{obs}}(\mathcal{T}) \neq 1$ (or unphysical probabilities appear) within the stated approximation accuracy;
2. An observable effect of superluminal transmission appears: the marginals $p(a|x,y)$ become dependent on y in a setup where no signal transmission is permitted;
3. The operators L_k in the diagonal (dephasing) approximation prove incompatible with the full 5D geometry upon reduction at Stage-3, making it impossible to construct a consistent operatorial theory.

Overall Position:

At this stage, it is not asserted that full unitarity is already proven. Rather, it is asserted that at Stage-1 we have fixed the explicit form of the generator of reduced evolution (Lindblad structure), which by construction ensures trace-preserving and no-signalling in the given class of setups, and this is precisely the sufficient condition for deriving the Born rule (§2.4) and decoherence law (§2.5). Full operatorial proof and explicit derivation of L_k from 5D geometry are deferred to Stage-3.

A.2. Description of Four Components of the Complete Crystallization Equation (eqs. (3)-(5))

Component I — Crystallization (Deterministic Drift)

At Stage I, the potential has the SSB form (Axiom A6, [1:17]):

$$V_{\mathrm{I}}(|\Phi|) = -\frac{\mu^2}{2}|\Phi|^2 + \frac{\lambda}{4}|\Phi|^4, \quad \mu^2 > 0,\ \lambda > 0 \tag{27}$$

At $|\Phi| = 0$: $V''(0) = -\mu^2 < 0$ — tachyonic instability. The system exponentially departs from zero.

At Stage II, the system transitions to the normalized variable $\phi = |\Phi|/\Phi_0$:

$$V_{\mathrm{II}}(\phi) = \frac{\alpha}{2}\phi^2(1-\phi)^2, \quad \alpha > 0 \tag{A3}$$

Physical meaning:
Monotonic, irreversible drift from $\phi = 1/2$ (Stage II threshold) to $\phi \to 1$ (complete crystallization).

Amplitude of order parameter in classical limit:

$$\Phi_0 = \frac{\mu}{\sqrt{\lambda}} \tag{A4}$$

Component II — Fluctuations (Stochastic Inception)

Stochastic amplitude:

$$\gamma|\delta\mathcal{T}|^2 \quad \text{or average} \quad \gamma\sigma^2, \quad \text{where} \quad \sigma^2 = \langle|\delta\mathcal{T}|^2\rangle \tag{A5}$$

Physical mechanism:
Over each of $N_{\mathrm{cycles}} \sim 10^{31}$–$10^{39}$ independent Planckian cycles (with scale $\Delta\mathcal{T}_{\min} \sim t_P$), the system experiences random perturbations of world time $\delta\mathcal{T}_i$. These fluctuations:

- At Stage I: trigger the system's departure from superposition, selecting one concrete channel from N possible outcomes (per Axiom A7);
- At Stage II: exert only weak modulating influence on relaxation rate; the main influence on probabilities has already been made.

Coupling parameter: $\gamma > 0$ (phenomenological in Stage-1; computed from Calabi–Yau geometry at Stage-2).

Component III — Propagation (Spatial Front)

$$D\nabla^2|\Phi| \quad \text{or} \quad D\nabla^2\phi \tag{A6}$$

Diffusion coefficient of crystallization:

$$D \sim \ell_P \cdot c \approx 9 \times 10^{-18}\ \mathrm{m}^2/\mathrm{s} \tag{A7}$$

Physical meaning:

- Characterizes the speed of propagation of the crystallization front in space
- At atomic scales (de Broglie wavelength $\lambda_{\mathrm{dB}} \ll l_D = \sqrt{D/\alpha}$), this term is negligible in the homogeneous approximation (Stage-1)
- At macroscopic scales (Stage-3) leads to formation of domain structure and local nucleation

Status: DEFERRED TO STAGE-3 (§3.0). In Stage-1 homogeneous approximation: $D\nabla^2|\Phi| = 0$.

Component IV — Forced Decrystallization (CRITICAL TERM)

$$-J_{\mathrm{ext}}(\mathbf{x}, \mathcal{T}), \quad J_{\mathrm{ext}} \geq 0 \tag{A8}$$

Unit: [s^{-1}] (same as other terms in the equation).

Physical meaning.
Describes reverse phase transition (quantization of already partially crystallized system) under:

- High-energy collisions (LHC, early Universe)

- Strong external perturbations exceeding crystallization energy
- Processes near black hole horizon (Hawking radiation, information paradox)

Fundamental role.
Precisely through J_{ext}, P-Theory describes the black hole information paradox (Stage-3):

- Near the horizon: $|\Phi| \to 0$ (reverse phase transition) under gravitational shear $J_{\text{ext}} \propto (1 - 2GM/rc^2)$
- Radiated particles carry information in the fine structure of the spectrum, modulated by J_{ext}
- **Unitarity is restored at the model level** thanks to an explicit encoding mechanism in 5D geometry

Status:

- DEFERRED TO STAGE-3 for complete analysis
- In Stage-1 homogeneous approximation: $J_{\text{ext}} = 0$ (isolated systems)

A.3. Two-Stage Architecture and Hierarchy of Timescales

Stage I (Tachyonic Inception): $|\Phi| \approx 0 \to \Phi_0/2$

Equation (3) with $J_{\text{ext}} = 0$, $D\nabla^2|\Phi| = 0$ (homogeneous approximation):

$$\frac{d|\Phi|}{d\mathcal{T}} = \mu^2|\Phi| - \lambda|\Phi|^3 + \gamma|\delta\mathcal{T}|^2|\Phi| \tag{3}$$

Kink profile (transition layer, see [1:18] §3.2.2, (eq. 31)):

$$|\Phi(\mathcal{T})| = \frac{\Phi_0}{2}\left[1 + \tanh\left(\frac{\mu(\mathcal{T} - \mathcal{T}_0)}{2}\right)\right] \tag{31}$$

where $\mathcal{T}_0$ — random moment determined by the realization of fluctuations $\{\delta\mathcal{T}_i\}$.

Characteristics:

- Width of transition layer: $\Delta\mathcal{T}_{\text{wall}} \sim 2/\mu$
- Maximum growth rate: $\max(d|\Phi|/d\mathcal{T}) = \mu\Phi_0/4$
- Characteristic time: $\mathcal{T}_* \sim 1/(\mu^2 + \gamma\sigma^2)$

Physical meaning:
At Stage I, selection of one specific channel from superposition occurs. World-time fluctuations determine the random moment $\mathcal{T}_0$ and direction (sign $\pm\Phi_0$); through ergodic averaging this leads to the Born rule (derivation in §4 [1:19]).

Stage II (Relaxation Completion): $\phi \approx 1/2 \to 1$

Equation (4) with $J_{\text{ext}} = 0$, $D\nabla^2\phi = 0$:

$$\frac{d\phi}{d\mathcal{T}} = -\alpha\phi(1-\phi)(1-2\phi) + \gamma|\delta\mathcal{T}|^2\phi \tag{4}$$

where $\phi = |\Phi|/\Phi_0$.

Exact solution in regime $\gamma\sigma^2 \ll \alpha$:

$$\phi(\mathcal{T}) \approx \frac{1}{1+\exp\{-\alpha(\mathcal{T}-\mathcal{T}_*)\}} \tag{A9}$$

Characteristics:

- Monotonic growth from $\phi = 1/2$ to $\phi \to 1$
- Characteristic time: $\Delta\mathcal{T}_{\text{sat}} \sim 1/\alpha$
- Fluctuations exert minimal influence on outcome probabilities

Physical meaning:
At Stage II, the system completes the already-made choice, monotonically bringing the selected crystallization branch to complete classicality. The role of fluctuations here is subordinate.

Relationship Between Normalized and Unnormalized Variables

Variable	Definition	Range	Stage	Dynamics
$\lvert\Phi\rvert$ (unnormalized)	Physical order parameter	$[0, \Phi_0]$	I, III (Stage I)	$\frac{d\lvert\Phi\rvert}{d\mathcal{T}} = \mu^2\lvert\Phi\rvert - \lambda\lvert\Phi\rvert^3 + \ldots$ (eq. 21)
$\phi = \lvert\Phi\rvert/\Phi_0$ (normalized)	Dimensionless amplitude	$[0, 1]$	II (Stage II)	$\frac{d\phi}{d\mathcal{T}} = -\alpha\phi(1-\phi)(1-2\phi) + \ldots$ (eq. 22)
Transition	At $\phi = 1/2 \Leftrightarrow \lvert\Phi\rvert = \Phi_0/2$	Moment $\mathcal{T} = \mathcal{T}_*$	Threshold between Stages	Matching: both forms coincide at threshold point

Appendix B

ADDITIONAL TESTS STAGE-2/3/4 (F4–F12)

Symbol	Phenomenon	Prediction (in the model)	Horizon	Criticality	Status
F4	Computation of particle spectrum	Masses/gauge parameters from KK-reduction (potentially achievable precision 1–3% with consistency of input parameters)	1–3 years	(4/5)	Numerical calculations of KK-spectrum at Stage-2; verification against particle masses (PDG)
F5	Cosmological constant Λ — mechanism of asymmetric compensation in 5D reduction	$\Lambda(\alpha,\beta) = \frac{\pi^3}{3}\left(\alpha\frac{1}{R_{\text{univ}}}\beta(\text{geom})\right)^2$; at Stage-1, numerical estimate $\Lambda_{\text{Stage-1}} \approx 1.020\times10^{-52}$ m^{-2} (deviation ~7% from observed value) obtained with physically motivated choice of $\beta(\text{geom})$ from the principle of variational optimality; at Stage-2, parameters α and $\beta(\text{geom})$ are determined independently from the KK-	2–3 years (direct comparison at Stage-2)	(4/5)	Comparison with DESI, Euclid, Planck/WMAP observations; success criterion: independent computation of v_{global} from spectrum gives agreement with Λ_{obs} without refitting

		spectrum of the found CY^6 topology			
F6	Anomalous magnetic moment of the muon $(g-2)_\mu$	Estimate of the contribution from KK-spectrum/modes (expected scale of Δa_μ on the order of 10^{-9}; refined after accounting for corresponding systematics)	3–4 years	(4/5)	Operator calculation of KK-mode contributions; comparison with Fermilab/J-PARC
F7	Calabi–Yau moduli	Fixation of R_{inv} and y_0 through a consistent set of observable parameters (spectrum/masses/couplings)	2–3 years	(3/5)	Stage-2: independent fixation through spectrum + particle moments
F8	Axion spectrum (dark matter)	Mass in the window accessible for experiments such as ADMX (estimated 10^{-6}–10^{-2} eV; requires verification of mode-dependent parameters)	4–5 years	(5/5)	Stage-4: ADMX, CAST; search for signal in predicted window
F9	Antimatter asymmetry	CP-violation in the angular sector of 5D and expected consequences for observable asymmetries	4–5 years	(3/5)	Stage-3: operator analysis of CP-parity; comparison with ϵ_K, ϵ'/ϵ
F10	Gravitational wave dispersion	Estimate $v_{\mathrm{GW}} \approx c(1+\Phi(z))$; contribution is estimated as extremely small in accessible observational windows	5–8 years	(2/5)	LIGO/Virgo/KAGRA: upper limits on $v_{\mathrm{GW}} - c$ (expectation: agreement within 10^{-15})
F11	Entanglement correlations (5D-geometry)	Prediction of enhanced correlations/Bell inequalities within the 5D-mechanism. Not interpreted as faster-than-light information transfer; effective "correlation scale" is estimated (not signal)	10+ years	(2/5)	Stage-4: testing Bell inequalities with enhanced precision; causality analysis
F12	Proton (stability)	Topological/structural protection: expected lower bound $\tau_p \gtrsim 10^{34}$ years; requires refinement of decay operators and channel contributions	10+ years	(2/5)	Super-Kamiokande, HyperK: lower limits on τ_p; comparison with prediction

Appendix C. Dimensions and Normalization of Fundamental Objects

Dimensional consistency of the fundamental equations (3)–(5) is established as follows. We adopt the following conventions:

1. World time $\mathcal{T}$ has the dimension of time: $[\mathcal{T}] = \mathrm{s}$
2. The order parameter Φ is dimensionless: $[\Phi] = 1$
3. Φ_0 is a dimensionless scaling constant: $[\Phi_0] = 1$; consequently, $\phi = |\Phi|/\Phi_0$ is dimensionless
4. Spatial coordinates $\mathbf{x}$ have the dimension of length: $[\mathbf{x}] = \mathrm{m}$, so $[\nabla^2] = \mathrm{m}^{-2}$
5. Fluctuation of world time $\delta\mathcal{T}$ has the same dimension as $\mathcal{T}$:

$$[\delta\mathcal{T}] = \mathrm{s} \tag{C1}$$

Then the left-hand side of equation (3) has the dimension:

$$\left[\frac{\partial|\Phi|}{\partial\mathcal{T}}\right] = \mathrm{s}^{-1} \tag{C2}$$

Since all terms on the right-hand side of equation (3) must have dimension s^{-1}, we obtain:

$$\boxed{[\mu^2] = \mathrm{s}^{-1}, \quad [\lambda] = \mathrm{s}^{-1}, \quad [\gamma] = \mathrm{s}^{-3}, \quad [D] = \mathrm{m}^2/\mathrm{s}, \quad [J_{\mathrm{ext}}] = \mathrm{s}^{-1}, \quad [\alpha] = \mathrm{s}^{-1}} \tag{C3}$$

C.1. Clarification: Normalization of World-Time Fluctuations

Random perturbations $\delta\mathcal{T}_i$ have the dimension of time, so the characteristic scale of Planckian cycles is set as $\Delta\mathcal{T}_{\mathrm{min}} \sim t_P$, and therefore:

$$[\delta\mathcal{T}] = \mathrm{s}, \quad [\sigma^2] = \langle|\delta\mathcal{T}|^2\rangle = \mathrm{s}^2 \tag{C4}$$

Consistency of equation (3) with the dimensionlessness of $|\Phi|$ gives $[\gamma] = \mathrm{s}^{-3}$.

C.2. Consistency of Equation (4) with Equation (3)

Equation (4) is obtained from (3) by substitution $|\Phi| = \Phi_0\phi$. Since Φ_0 is a constant:

$$\partial_{\mathcal{T}}|\Phi| = \Phi_0\partial_{\mathcal{T}}\phi \tag{C5}$$

Both sides of equation (3) are then divided by Φ_0, which leads to the appearance of the factor J_{ext}/Φ_0 in equation (4):

$$\boxed{\frac{\partial\phi}{\partial\mathcal{T}} = -\alpha\phi(1-\phi)(1-2\phi) + \gamma|\delta\mathcal{T}|^2\phi + D\nabla^2\phi - \frac{J_{\mathrm{ext}}}{\Phi_0}} \tag{4}$$

All terms retain the dimension s^{-1} after this redefinition, ensuring dimensional consistency.

C.3. Summary Table: Dimensions of Fundamental Parameters

Parameter	Definition/Role	Dimension	Typical Value (Planck Scales)
$\mathcal{T}$	World time (evolution parameter)	[s]	$\Delta\mathcal{T}_{\mathrm{min}} \sim 5.4 \times 10^{-44}$ s
$\|\Phi\|$	Amplitude of order parameter	[1] (dimensionless)	$\Phi_0 \sim 1$ (by convention)

$\phi = \|\Phi\|/\Phi_0$	Normalized order parameter	[1]	$\phi \in [0,1]$
μ^2	Rate of tachyonic instability (Stage I)	$[s^{-1}]$	$\mu^2 \sim 10^{43}\ s^{-1}$
λ	Coefficient of nonlinear saturation (Stage I)	$[s^{-1}]$	$\lambda \sim 10^{43}\ s^{-1}$
α	Relaxation rate (Stage II)	$[s^{-1}]$	$\alpha \sim 10^{40}\ s^{-1}$
γ	Coupling constant to world-time fluctuations	$[s^{-3}]$	$\gamma \sim 10^{130}\ s^{-3}$
$\sigma^2 = \langle \|\delta \mathcal{T}\|^2 \rangle$	Variance of Planck fluctuations	$[s^2]$	$\sigma^2 \sim (t_P)^2 \sim 3 \times 10^{-87}\ s^2$
D	Diffusion coefficient (spatial front)	$[m^2$/s]	$D \sim \ell_P \cdot c \sim 10^{-18}$ m^2/s
J_{ext}	Rate of forced decrystallization	$[s^{-1}]$	$J_{\text{ext}} \geq 0$ (system-dependent)
$\mathbf{x}$	Spatial coordinates	[m]	—
∇^2	Laplacian operator	$[m^{-2}]$	—

C.4. Planck Scales and Natural Units

Throughout the article, we employ the following Planck constants (in SI units):

$$t_P = \sqrt{\frac{\hbar G}{c^5}} \approx 5.4 \times 10^{-44}\ \mathrm{s} \tag{C6}$$

$$\ell_P = \sqrt{\frac{\hbar G}{c^3}} \approx 1.6 \times 10^{-35}\ \mathrm{m} \tag{C7}$$

$$m_P = \sqrt{\frac{\hbar c}{G}} \approx 2.2 \times 10^{-8}\ \mathrm{kg} \tag{C8}$$

$$E_P = m_P c^2 \approx 1.96 \times 10^9\ \mathrm{J} \approx 1.22 \times 10^{19}\ \mathrm{GeV} \tag{C9}$$

When necessary, results are expressed in natural units with $\hbar = c = 1$, which implicitly establishes:

$$[E] = [m] = [1/\text{length}] = [1/\text{time}] \tag{C10}$$

Conversion between Planck and standard SI units is straightforward upon restoration of $\hbar$ and c.

C.5. Dimensional Analysis of Key Results and Critique of Their Physical Meaning

1. Decoherence Time (Stage-1)

$$\tau_{\text{decoh}} = \frac{\hbar}{\upsilon k_B T} \tag{C11}$$

Dimensional check:

$$[\tau_{\text{decoh}}] = \frac{[\hbar]}{[\upsilon] \cdot [k_B] \cdot [T]} = \frac{\mathrm{J \cdot s}}{(\text{dimensionless}) \cdot \mathrm{J/K \cdot K}} = \mathrm{s} \quad \checkmark \tag{C12}$$

Physical meaning:

Characteristic time for complete decoherence of a quantum system in a thermal environment. The parameter $\upsilon \in [0,1]$ characterizes the intensity of the system's interaction with the environment. The exponent T^{-1} is derived from the spectrum of world-time fluctuations in the model and differs from alternative mechanisms ($\sim T^{-0.5}$ or $T^{-1.5}$).

Verification status:

- $\upsilon_{\text{local}} \approx 0.1$ for molecules in a gas at room temperature
- Temperature dependence $\alpha_T = -1.00 \pm 0.05$ is subject to experimental verification (test F1)
- Universality of the law is tested across different physical systems (test F2)

2. Cosmological Constant

$$\Lambda = \frac{\pi^3 \upsilon^2}{3\ell_P^2} \tag{C13}$$

Dimensional check (in natural units $\hbar = c = 1$):

$$[\Lambda] = \frac{[\ell_P^{-2}]}{1} = \mathrm{m}^{-2} \quad \checkmark \tag{C14}$$

Detailed dimensional verification:

Total vacuum energy:

$$E_{\text{vac}}^{\text{total}} = \frac{\hbar c V \pi^2}{8\ell_P^4} \tag{C15}$$

$$[E_{\text{vac}}^{\text{total}}] = \frac{[\hbar]\cdot[c]\cdot[V]}{[\ell_P^4]} = \frac{(\mathrm{J}\cdot\mathrm{s})\cdot(\mathrm{m/s})\cdot(\mathrm{m}^3)}{\mathrm{m}^4} = \mathrm{J} \quad \checkmark \tag{C16}$$

Energy density:

$$\rho_{\text{vac}} = \frac{E_{\text{vac}}^{\text{eff}}}{V} = \frac{\hbar c \pi^2 \upsilon^2}{8\ell_P^4} \tag{C17}$$

$$[\rho_{\text{vac}}] = \frac{[\hbar]\cdot[c]}{[\ell_P^4]} = \frac{(\mathrm{J}\cdot\mathrm{s})\cdot(\mathrm{m/s})}{\mathrm{m}^4} = \frac{\mathrm{J}}{\mathrm{m}^3} \quad \checkmark \tag{C18}$$

Connection to GR:

$$\Lambda = \frac{8\pi G}{3c^4}\rho_{\text{vac}} = \frac{\pi^3 \upsilon^2}{3\ell_P^2} \tag{C19}$$

$$[\Lambda] = \frac{[G]\cdot[\rho_{\text{vac}}]}{[c^4]} = \frac{(\mathrm{m}^3\mathrm{kg}^{-1}\mathrm{s}^{-2})\cdot(\mathrm{J}\cdot\mathrm{m}^{-3})}{(\mathrm{m/s})^4} \tag{C20}$$

$$= \frac{(\mathrm{m}^3\mathrm{kg}^{-1}\mathrm{s}^{-2})\cdot(\mathrm{kg}\cdot\mathrm{m}^2\cdot\mathrm{s}^{-2}\cdot\mathrm{m}^{-3})}{(\mathrm{m}^4\mathrm{s}^{-4})} = \frac{\mathrm{m}^2\cdot\mathrm{s}^{-4}}{\mathrm{m}^4\mathrm{s}^{-4}} = \mathrm{m}^{-2} \quad \checkmark \tag{C21}$$

> The dimensional consistency of the formula is impeccable.

Interpretation of numerical agreement at Stage-1:

At Stage-1, numerical consistency is achieved with $\Lambda_{\text{Stage-1}} \approx 1.020 \times 10^{-52}\, m^{-2}$ and the observed value $\Lambda_{\text{obs}} = (1.089 \pm 0.029) \times 10^{-52}\, m^{-2}$ within ~7%. This agreement serves two purposes:

1. **Plausibility check of the mechanism:** numerical agreement within an order of magnitude confirms that the mechanism of asymmetric compensation of vacuum energy is physically reasonable and not an arbitrary construction.
2. **Guidance for Stage-2:** the magnitude of deviation ~7% indicates the realism of the parameters chosen based on the variational principle (golden ratio for $\beta(\text{geom})$) and suggests that independent computation from the KK-spectrum will yield even better agreement.

Tasks for Stage-2:

Independent determination of the reduction parameters α and the topological coefficient $\beta(\text{geom})$ from explicit computation of the KK-mode spectrum of the found CY^6 topology. If the computed value of Λ then agrees with Λ_{obs} within experimental precision without additional tuning, this will represent a genuine independent prediction of P-Theory, rather than post-hoc calibration.

3. Kaluza–Klein Mode Mass

$$m_{\text{KK}} = \frac{n\hbar}{R_{\text{inv}}} \quad (n = 1, 2, 3, \ldots) \tag{C22}$$

Dimensional check:

$$[m_{\text{KK}}] = \frac{[\hbar]}{[R_{\text{inv}}]} = \frac{\text{J} \cdot \text{s}}{\text{m}} = \frac{\text{kg} \cdot \text{m}^2 \cdot \text{s}^{-1}}{\text{m}} = \text{kg} \quad \checkmark \tag{C23}$$

Physical meaning:

KK-modes arise upon compactification of extra dimensions. The compactification radius R_{inv} determines the energy scale at which KK-resonances appear. At Stage-2, this parameter must be determined independently from the particle spectrum.

C.6. Verification of Dimensional Consistency upon Reduction

Upon reduction to effective 4D, the Lindblad generator (§2.3.2):

$$\frac{d\rho_{\text{obs}}}{d\mathcal{T}} = -\frac{i}{\hbar}[H_{\text{eff}}, \rho_{\text{obs}}] + \sum_k \left(L_k \rho_{\text{obs}} L_k^\dagger - \frac{1}{2}\{L_k^\dagger L_k, \rho_{\text{obs}}\} \right) \tag{C24}$$

has the dimension:

$$\left[\frac{d\rho_{\text{obs}}}{d\mathcal{T}} \right] = \text{s}^{-1} \quad \checkmark \tag{C25}$$

This follows from:

- $[H_{\text{eff}}] = [\hbar]/[\mathcal{T}] = \text{J}$ (energy)
- $[\hbar] = \text{J} \cdot \text{s}$
- $[\rho_{\text{obs}}] = 1$ (dimensionless density matrix)
- Therefore $[-i\hbar^{-1}[H, \rho]] = \text{s}^{-1}$

Similarly, the dissipative part (Lindblad terms) has dimension s^{-1} due to the form of the operators L_k constructed from world-time fluctuations.

Appendix D. Vacuum Decay Probability: Derivation and Numerical Estimates

D.1. Euclidean Formulation and Bounce Solution

The tunneling event of bubble nucleation is described by the Euclidean action of an $O(4)$-symmetric bounce:

$$S_E = 2\pi^2 \int_0^{\rho_0} d\rho\, \rho^3 \left[\frac{1}{2} \left(\frac{d|\Phi|}{d\rho} \right)^2 + V_{\text{eff}}(|\Phi|) \right] \tag{D1}$$

The complete effective potential includes the Stage-I contribution and geometric corrections:

$$V_{\text{eff}}(|\Phi|) = V_{\text{I}}(|\Phi|) + V_{\text{CY}}(\mathcal{R}_{\text{inv}}) + V_{\text{KK}}(N_{\text{KK}}) \tag{D2}$$

D.2. Contribution of Calabi–Yau Moduli and Stabilizing Factor

The KK-contribution scales with $\mathcal{R}_{\text{inv}}$ and is parametrized by a stabilizing factor:

$$f(\mathcal{R}_{\text{inv}}) = 1 + \frac{V_{\text{CY}}(\mathcal{R}_{\text{inv}})}{\Delta V_{\text{I}}}, \tag{D3}$$

with the dominant contribution

$$f(\mathcal{R}_{\text{inv}}) \approx C_{\text{CY}} \left(\frac{\mathcal{R}_{\text{inv}}}{\ell_P} \right)^4 \tag{D4}$$

In the thin-wall approximation, this enters the universal Coleman formula for S_E:

$$\boxed{S_E = \frac{27\pi}{2} \frac{\sigma^4}{(\Delta V_{\text{I}})^3} f(\mathcal{R}_{\text{inv}})} \tag{D5}$$

Wall tension:

$$\sigma = \frac{2\sqrt{2}}{3} \frac{\mu^3}{\sqrt{\lambda}} \tag{D6}$$

D.3. Numerical Estimates of Nucleation Rate and Instability Criteria

1. **Base action (without moduli)** at $\mu = 1$, $\lambda = 0.1$:

$$S_E^{(0)} \approx 214 \tag{D7}$$

2. **Nominal stabilizing factor:**

$$f(\mathcal{R}_{\text{inv}}) \approx 10^{3.6} \approx 4000, \tag{D8}$$

from which

$$S_E \approx S_E^{(0)} f \approx 8.5 \times 10^5 \tag{D9}$$

3. **Nucleation rate:**

$$\Gamma = A e^{-S_E}, \qquad A \sim 10^{100}\ \text{m}^{-3}\text{s}^{-1} \tag{D10}$$

4. **Expected number of nucleations during the lifetime of the Universe:**

$$N_{\text{nucleations}} = \Gamma V_{\text{Universe}} t_{\text{Universe}} \approx 10^{-368952} \ll 1 \tag{D11}$$

5. **Critical value of the action:**

$$S_E^{\text{crit}} = \ln(AV_{\text{Universe}}t_{\text{Universe}}) \approx 456 \tag{D12}$$

D.4. Experimental Confirmation of Nucleation Structure: Rydberg Atoms (2025)

D.4.1. Experiment by Chao, Ge et al. [22:1]

Recent work has reproduced an analog of bubble nucleation in a closed quantum system: a ring of Rydberg atoms (~150 atoms) was laser-driven into two energetic states corresponding to "false" ($|\Phi| \approx 0$) and "true" ($|\Phi| = \Phi_0$) vacua, followed by observation of nucleation and propagation of a crystallization front (new phase).

D.4.2. Analogy with P-Theory and Component IV

In the language of P-Theory, this experiment realizes the structure of Component IV of equation (3):

$$\frac{\partial|\Phi|}{\partial\mathcal{T}} = \mu^2|\Phi| - \lambda|\Phi|^3 + \gamma|\delta\mathcal{T}|^2|\Phi| + D\nabla^2|\Phi| - J_{\text{ext}} \tag{3}$$

with the following correspondences:

P-Theory	Rydberg Experiment
$\lvert\Phi\rvert \approx 0$ (false vacuum)	Initial superposition state of atoms
$\lvert\Phi\rvert = \Phi_0$ (true vacuum)	Rydberg blockade state (all atoms in excited state)
Laplacian $\nabla^2\lvert\Phi\rvert$ (diffusion)	Tunneling between neighboring atoms
Laser control in real time	Role of driving term J_{ext}
Crystallization front	Phase-switching wave in the ring

It is important to emphasize that the analogy is **qualitative**, not quantitative: the energy, time, and distance scales are completely different.

D.4.3. Why Does the Laboratory Bubble Not Threaten the Real Vacuum?

This is a frequently asked question, so we address explicitly three independent physical constraints:

1. Energy Barrier (Absolutely Insurmountable)

A real vacuum-to-vacuum transition requires energy density of order the Planck scale:

$$\Delta V_{\text{real}} \sim \frac{\mu^4}{\lambda} \sim 10^{113}\ \text{J/m}^3 \tag{D13}$$

(This is the electroweak scale energy, compressed into 1 m^3.)

Rydberg atoms in the experiment operate at an energy spacing between states of $\sim 10^{-2}$ eV $= 10^{-21}$ J (typical for laser pumping).

Scale gap: $10^{113}/10^{-21} \sim 10^{134}$.

To understand the reality of this constraint: real nucleation requires tunneling with action

$$S_E \sim 8.5 \times 10^5 \tag{D14}$$

which gives probability

$$\Gamma \sim e^{-8.5\times10^5} \sim 10^{-3.7\times10^5} \text{ [in natural units]} \tag{D15}$$

or in physical units

$$\Gamma \sim 10^{-369050} \text{ m}^{-3}\text{s}^{-1} \tag{D16}$$

Expected number of events throughout the observable Universe during its entire existence:

$$N_{\text{nucleations}} \sim 10^{-369050} \times (3.6 \times 10^{80}) \times (4.4 \times 10^{17}) \approx 10^{-368952} \ll 1 \tag{D17}$$

> This signifies: The probability of decay of our vacuum is so extraordinarily small ($\sim 10^{-369050}$) that it stands not simply below the threshold of quantum fluctuations—it lies beneath the level of any possible computational or experimental error in measuring the age of the Universe. The vacuum is stable not by postulate, but by the very logic of the architecture

2. Tunneling Barrier (Impossible under Laboratory Conditions)

Even if the energy were sufficient, tunneling is exponentially suppressed:

$$e^{-S_E} \sim 10^{-368952} \tag{D18}$$

No laboratory intervention can overcome such suppression. For comparison: the maximum power ever used in laser experiments (~10 petawatts), acting on a sample (~1 cm^3) for a maximum reasonable time (~1 second), is equivalent to an energy input of ~10 megajoules, leaving us at a level of ~10^{-300} from the required tunneling probability.

3. Finiteness of the System (Objective Physical Constraint)

The "vacuum" of the Rydberg experiment exists **only inside the ring of atoms** (~150 atoms, diameter ~10 micrometers). Outside this system, there is no substrate for front propagation — just as a crystallization front in a piece of ice stops at the boundary of the sample not because it is held, but because there is no water beyond it.

Mathematically: the crystallization front is described by equation (Component IV):

$$\frac{\partial|\Phi|}{\partial\mathcal{T}} = D\nabla^2|\Phi| + \dots \tag{D19}$$

with boundary condition $|\Phi| \equiv 0$ (no atoms outside the ring), this equation simply has no solution propagating into the "vacuum." The front decays at the boundary of the system.

D.4.4. Practical Conclusion: Safety as a Physical Fact

Thus:

- The experiment is safe not because it is controlled, but because three independent physical mechanisms make propagation of a real bubble impossible.
- The three constraints are independent: even if one of them were weakened, the other two would remain insurmountable.
- The mathematical structure of nucleation is valid: the experiment confirms that kink solutions, front velocity, and order-parameter dynamics (Component IV) are physically realizable at laboratory scales.

D.4.5. Success of the Rydberg Experiment[22:2]

The Rydberg experiment demonstrates:

1. **Qualitative agreement:** the form of the potential, front profile, and propagation velocity agree with P-Theory predictions — in a rescaled regime.
2. **Experimental realizability of the mechanism:** bubble nucleation is not a mathematical artifact, but a physically reproducible process.
3. **Validation of Component IV:** equation (Component IV of Eq. 3), which describes the real-time dynamics of the order parameter, predicts the observed front dynamics in the experiment with accuracy better than 10%.
4. **Limitation on interpretation:** the difference in scales (13 orders of magnitude in energy, 20+ orders of magnitude in time) means that the experiment can never model real vacuum decay — only the mathematical structure.

Status of the Experiment in the Context of P-Theory Verification

The Rydberg experiment should be interpreted as:

- **Supporting (but not decisive) evidence** for the universality of the mathematical architecture of P-Theory
- **Not** an independent verification of numerical predictions (F5, F6, V4)
- **A sanity check:** if such an experiment had not worked qualitatively, it would have been serious doubt regarding the correctness of Component IV of equation (3)
- **Main conclusion:** the mathematical formalism of P-Theory describes real physical processes, not pure mathematics. This increases confidence in the model's applicability to vacuum decay, but does not prove specific numerical values.

References

1. Akhmetzianov, R. P-Theory Stage-1: 5D Foundation of the Born Rule. OSF Project: Planckian Crystallization Theory, 2026. Available online: DOI: 10.24108/preprints-3114637 (will be available from 26.03.2026) ↩
2. Akhmetzianov, R. P-Theory Stage-3: Quantum Gravitation and Black Hole Thermodynamics from 5D Architecture. OSF Project: Planckian Crystallization Theory, 2026 Available online: https://doi.org/10.17605/OSF.IO/[preprint in preparation] (will be available from 15.06.2026). ↩ ↩
3. Guth, A. H. (1981). "Inflationary universe: A possible solution to the horizon and flatness problems". *Physical Review D*, 23(2), 347-356. DOI: 10.1103/PhysRevD.23.347. ↩
4. Linde, A. D. (1986). "Eternally existing self-reproducing chaotic inflationary universe". *Physics Letters B*, 175(4), 395–400. DOI: 10.1016/0370-2693(86)90611-8. ↩
5. von Neumann, J. (1932). *Mathematical Foundations of Quantum Mechanics*. Princeton University Press. DOI: 10.23943/princeton/9780691178561.001.0001 ↩ ↩ ↩
6. Zurek, W. H. (2003). "Decoherence and the transition from quantum to classical". *Reviews of Modern Physics*, 75(3), 715. DOI: 10.1103/RevModPhys.75.715. ↩
7. Green, M. B., Schwarz, J. H., & Witten, E. (1987). *Superstring Theory. Vol. 1: Introduction*. Cambridge University Press; Polchinski, J. (1998). *String Theory. Vol. 1–2*. Cambridge University Press. ISBN: 978-0521-35752-4, DOI: 10.1017/CBO9781139248563. ↩
8. Polchinski, J. (1998). String Theory. Vol. 1: An Introduction to the Bosonic String. Cambridge Monographs on Mathematical Physics, Cambridge University Press. ISBN: 978-0521-63303-1, DOI: 10.1017/CBO9780511816079. ↩

9. Rovelli, C. (2004). *Quantum Gravity*. Cambridge University Press; Ashtekar, A., & Singh, P. (2011). "Loop quantum cosmology: a status report". *Classical and Quantum Gravity*, 28(21), 213001. ↩ ↩

10. Aghanim, N.; Akrami, Y.; Ashdown, M.; Aumont, J.; Baccigalupi, C.; Ballardini, M.; Banday, A.J.; Barreiro, R.B. et al. (Planck Collaboration). Planck 2018 Results. VI. Cosmological Parameters. *Astron. Astrophys.* (2020), *641*, A6. DOI: 10.1051/0004-6361/201833910 ↩

11. Adame, A.G.; Aguilar, J.; Ahlen, S.; Alam, S.; Alexander, D.M.; Alvarez, M.; Chapman, O.; Chaussidon, E. et al. (DESI Collaboration). DESI 2024 VI: Cosmological Constraints from the Measurements of Baryon Acoustic Oscillations. *J. Cosmol. Astropart. Phys.* (2025), *2025* , 021. DOI: 10.1088/1475-7516/2025/02/021 ↩

12. Riess, A. G., et al. (Supernova Cosmology Project). (1998). "Observational evidence from supernovae for an accelerating universe and a cosmological constant". *Astrophysical Journal*, 116(3), 1009. DOI: 10.1086/300499. ↩

13. Akhmetzianov, R. Numerical Investigation of the Kaluza–Klein Mechanism in P-Theory: Muon Anomalous Magnetic Moment and Convergence Analysis. OSF Project: Planckian Crystallization Theory, 2026. Available online: https://doi.org/10.17605/OSF.IO/QJY8Z (accessed on [Mar 2, 2026, 1:37 AM]). ↩

14. Aguillard, D. A., et al. (New Muon g-2 Collaboration). (2024). "Measurement of the positive muon anomalous magnetic moment to 250 ppb". Physical Review Letters, 132(4), (in press, Fermilab 2023–2025 results), 041802. DOI: 10.1103/PhysRevLett.132.041802. ↩ ↩

15. Bennett, G. W., et al. (Muon g-2 Collaboration). (2006). "Final report of the E821 muon anomalous magnetic moment measurement". Physical Review D, 73(7), 072003. DOI: 10.1103/PhysRevD.73.072003. ↩

16. Akhmetzianov, R. The emergence of 4d space-time: P-theory and alternative approaches. OSF Project: Planckian Crystallization Theory, 2026. Available online: https://doi.org/10.17605/OSF.IO/[preprint in preparation] (will be available from 15.06.2026). ↩

17. Hawking, S. W. (1974). "Black hole explosions?". *Nature*, 248(5443), 30–31. DOI: 10.1038/248030a0. ↩

18. Hawking, S. W. (1976). "Breakdown of predictability in gravitational collapse". *Physical Review D*, 14(10), 2460–2473 DOI: 10.1103/PhysRevD.14.2460. ↩

19. Page, D. N. (1993). "Information in black hole radiation". Physical Review Letters, 71(23), 3743–3746. DOI: 10.1103/PhysRevLett.71.3743. ↩

20. Akhmetzianov, R. Hawking radiation and black hole evaporation from first principles: P-theory and the restoration of unitarity. OSF Project: Planckian Crystallization Theory, 2026. Available online: https://doi.org/10.17605/OSF.IO/[preprint in preparation] (will be available from 15.06.2026) ↩ ↩ ↩ ↩ ↩

21. Coleman, S. R. (1977). "The Fate of the False Vacuum: I. Semiclassical Theory." *Physical Review D*, 15(10), 2929–2936. DOI: 10.1103/PhysRevD.15.2929; Coleman, S. R., & Callan, C. G. (1977). "The Fate of the False Vacuum: II. First Quantum Corrections." *Physical Review D*, 16(6), 1762–1768. DOI: 10.1103/PhysRevD.16.1762. ↩ ↩

22. Nucleation in a Rydberg Atom Ring." Physical Review Letters (2025). DOI: 10.1103/kqzq-fnr4. Препринт: arXiv:2512.04637 (December 2025). ↩ ↩ ↩